Earthline Journal of Chemical Sciences
E-ISSN: 2581-9003; CODEN: EJCSB4
Volume 11, Number 3, 2024, Pages 323-377
https://doi.org/10.34198/ejcs.11324.323377

Some CL-20 based energetic cocrystals - A review

Lemi Türker

Department of Chemistry, Middle East Technical University, Üniversiteler, Eskişehir Yolu No: 1, 06800 Çankaya/Ankara, Turkey; e-mail: lturker@gmail.com; lturker@metu.edu.tr

Abstract

There exists an inherent contradiction between the energy density and safety of energetic materials. To ameliorate and get an accord between energy and safety, cocrystallization seems to be a remedy which has been getting quite popular in the field of energetic materials. Energetic cocrystals represent one of the most important classes of research advances in the area of energetic materials. The cocrystallization significantly improves performance of energetic cocrystals, such as density, solubility, sensitivity, and thermal stability. This mini review summaries some of CL-20 based energetic cocrystals in terms of various aspects of them.

Introduction

Generally, more reaction steps and a longer processing period is required for the synthesis of novel energetic materials (EMs) in order to modify or ameliorate their ballistic properties (especially note the contradiction between the energy density and safety of energetic materials). In other words, this type of approach is an extremely complicated and time-consuming, often hazardous process. Another approach could be crystal modifications (such as coating and doping), by means of which the sensitivity of EMs is reduced. However, they suffer from energy losses and limited applicability areas. To overcome this problem, cocrystallization technology has been usually applied in the field of EMs in order to get better balance between the energy and safety. Cocrystallization could be mainly of two types; energetic-energetic or energetic-nonenergetic energetic cocrystals (ECCs) for the purpose of achieving different aims. Hence, the starting point is to choose the suitable components of the cocrystal.

Received: April 11, 2024; Accepted: May 18, 2024; Published: May 30, 2024

Keywords and phrases: cocrystal, HNIW, CL-20, explosive, nitramine.

CL-20, which is also known as 2,4,6,8,10,12-hexanitro-2,4,6,8,10,12-hexaaza-tetracyclo-[5.5.0.05,9.03,11]-dodecane (HNIW), falls in to the class of nitramine-type energetic materials [1-3].

HNIW

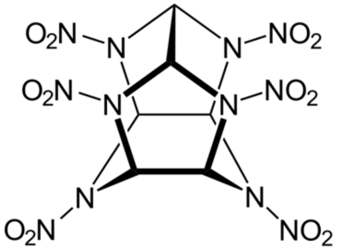

Nitramines (acyclic, cyclic, caged etc.) constitute an important class of explosive materials which include the explosives, propellants, and pyrotechnics [1-4]. CL-20 is a caged-type nitramine [5,6]. CL-20, is often found in these energetic-energetic type cocrystals. It is worth mentioning that CL-20 is currently the most powerful commercially available explosive, thus making it a major focus of cocrystallization efforts.

Through the centuries, synthesis or some research on EMs has evolved relatively slowly, due to the many reasons or difficulties have been encountered. Namely the synthesis of novel EMs possesses some drawbacks which may include many reaction steps and a longer processing period, etc. They were multiple and strict requirements for application (e.g., keeping safety, increasing energy, lowering cost, improving mechanic and ballistic properties, promoting environmental adaptability, etc.), intrinsic energy-safety contradiction of EMs themselves, in addition to risk of undesired and accident hurt, inadequate devotion, and so forth [7,8]. The key performance factors for EMs include the criteria of oxygen balance, density, thermal stability, sensitivity, and detonation parameters [9]. However, for some highly EMs, it is always difficult to keep the high energy content in accord with acceptable sensitivity, which is an intractable problem to be solved for better/longer storage, easy and safe transportation, handling and applications. Therefore, it is essential to find solution to this balance problem between energy density and sensitivity. Various strategies have been explored in the past years (such as design and synthesis of new EMs) with the help of inspiration drawn from modern science and technology, [10,11] improvement of crystal quality, [12] the fine coating of energetic particles, [13] and doping of energetic composites with a minor inert material [14].

Nowadays there has been a huge demand and challenge to overcome these difficulties to create novel EMs, which are both energetic and safe but meantime less hazardous to environment. The cocrystallization concept as a very promising strategy, has been a recent introduction to EMs. Cocrystallization is now changing the idea for creating new EMs, with producing more and more energetic cocrystals (ECCs) coming into scène, being as promising alternatives to synthesizing novel energetic molecules. Note that the principle idea of cocrystallization is to arrange heterogeneous molecules orderly in lattice with fixed stoichiometric properties [15-19].

The cocrystallization technique for EMs has attracted much attention, and it basically involves the rearrangement of different molecules at a molecular level, which consequently and efficiently vary various properties, including ballistic ones such as reducing the mechanical sensitivity without greatly sacrificing the energy density [20]. Cocrystallization refers to the orderly control and regulation of two or more different component crystals at the molecular level, so that eventually forming uniform cocrystals. Thus, the components of an ECC can be already existent energetic molecules, instead of newly synthesized novel ones necessarily. Hence, by means of the modification of cocrystallization, it is possible to make even some energetic compounds with the existing EMs but are already out of use (dead) come back to life having properties more apt to application [21]. These dead energetic compounds generally suffer one or more fatal shortcomings such as very high sensitivity, highly hazardous to environment and ready to be hydrolyzed.

Note that by definition a cocrystal refers to a single phase crystalline solid composed of two or multiple components in a proper stoichiometric ratio, and the components of a cocrystal can be atoms, molecules, anions and cations in pairs, and/or metallic cations with free electrons shared [22]. In recent years, cocrystallization had become a hot focus for researchers, based on the kinds of their components. Their interactions in crystal entity may include atomic cocrystal, molecular cocrystal, ionic cocrystal, metallic cocrystal and mixed-type cocrystal [22]. It had been applied extensively as an effective method in order to alter the oxygen balance (OB), molecular structure, density, improve mechanical properties, decrease sensitivity, increase detonation performance and enhance thermal stability of energetic materials.

An energetic cocrystal (ECC) refers to a crystalline structure that contains at least two components and at least one energetic component and energetic hydrates and other solvates [21,22]. Note that since non-energetic coformers will dilute energetic density, the energetic-energetic cocrystals (EECCs) whose components are both energetic are favored.

Compared with the other modification methods, cocrystallization can change the internal compositions and crystal structures of EMs without destroying the bonding structure of the original energetic compounds [23]. In the past decades, cocrystallization technology has been extensively used in pharmaceutical chemistry [24]. Beyond pharmaceutical materials, nowadays cocrystallization has also been developed as a common and efficient technique in the field of EMs.

It is worth mentioning that in cocrystals generally, the combination of two or more different molecules occurs in the same crystal lattice with a fixed stoichiometric ratio through strong intermolecular interactions, hence forming a unique multicomponent single crystal [25]. However, in recent years, some other definitions slightly different from each other have emerged in the literature one after another. The most commonly used definition in the pharmaceutical field is that "cocrystals are solids that are crystalline single phase materials composed of two or more different molecular and/or ionic compounds generally in a stoichiometric ratio which are neither solvates nor simple salts" [26]. An extended and more popular definition of cocrystal is that "a cocrystal is a single-phase crystalline solid composed of two or multiple components at a stoichiometric ratio, and the components of a cocrystal can be atoms, molecules, anions and cations in pairs, and/or metallic cations with free electrons shared" [22]. On the other hand, an energetic cocrystal (as the product of cocrystallization) refers to a cocrystal that contains at least one energetic component. Note that not only a molecule but also an ion can be cocrystallized to form energetic cocrystals in order to get modified properties [27].

Note that a reliable theoretical basis is still lacking for the experiments on preparation of cocrystals. Because of the fact that the corresponding formation mechanisms are still not clear, and hence the theoretical design method is not yet reliable [28]. In addition, the current preparation techniques for energetic cocrystals have a high risk of producing unwanted/undesirable structures, especially when the crystallization components and solvent systems used are complicated. The most important problem originates from the fact that there are just a few studies involving the cocrystal composition-structure-performance correlations, which could be too complicated to be clarified. Besides these problems, few researchers have explored the combustion and explosion mechanisms of HMX-based and CL-20-based energetic cocrystals, resulting in insufficient understanding of the energy release process of these types of EMs, which severely limits their any industrial applications [28].

Although, any theoretical design methods have not been reliable yet [28] it has been demonstrated by Shan and Zaworotko that the energetic/energetic cocrystals (EECCs) can reduce energy dissipation more effectively than an energetic/nonenergetic cocrystal [29]. Note that stronger intermolecular interactions between the components of cocrystal are responsible for the emergence of higher insensitivity.

It is worth mentioning that the stability of the cocrystal system is maintained via noncovalent interactions, such as hydrogen bonding, p-π stacking, π-π stacking, and halogen bonds. Their formation causes changes in intermolecular interactions rather than intramolecular covalent bonding. To a large extent, intermolecular interactions determine the structure and properties of the ECCs. This is also true for single-component energetic crystals. For instance, the strong intermolecular hydrogen bonding [30] in FOX-7 and TATB is an important factor that leads to the occurrence of insensitivity behavior. It is also known that planar conjugated molecular structures supporting π-π stacking may result in elevated impact energies for initiation [31].

Also, due to their strong, specific and directional nature, hydrogen and halogen bonds have gained extensive attention [28]. For instance, HMX molecules combined with DMF molecules mainly through four intermolecular hydrogen bonds in the HMX/DMF cocrystal. Molecules with H-donors and acceptors can easily form ECCs via forming hydrogen bonds [32]. The nitrogen atoms in the $-NO_2$ groups of CL-20 molecules can form intermolecular hydrogen bonds with the hydrogen atoms in $-NH_2$ groups of two nitroguanidine (NQ) molecules [33].

In some cases p-π interactions are observed as one of the dominant interactions in the cocrystals. In p-π interactions, p and π refer to the p-electrons of the NO_2 groups and the π-electrons of the coformer molecules, respectively. In fact, the p-π interactions comprise the sum of electrostatic and van der Waals ones. In addition, the O/H intermolecular interaction plays an important role in the structure of cocrystals. For instance, the hydrogen bond is stronger where HMX or CL-20 is considered as the hydrogen donor. On the other hand, π-π stacking could be found in aromatic energetic compounds such as 2,4,6-trinitrotoluene (TNT), which can form a number of cocrystals with conjugated structures [34].

Cocrystal explosives

Cocrystal explosives have been synthesized in a variety of ways, including the solvent evaporation, spray drying, vacuum freeze-drying, ball milling, electron spray deposition, self-assembly, and so on. Liu *et al.*, [35] prepared hexanitrohexaazaisowurzane (CL-20)/DNDAP cocrystals by employing the slow evaporation and spray drying methods. Nano-CL-20/1,3,5,7-tetrachitro-1,3,5,7-tetrachitroheterocyclic octane (HMX) and CL-20/2,4-DNI cocrystals were prepared also by spray drying method [36,37]. Gao *et al.*, [33] applied the vacuum freeze-drying method to prepare nano-CL20/NQ Cocrystal. On the other hand, Qiu *et al.,* [38] synthesized nanoscale CL-20/HMX high explosive cocrystal by the bead milling technique. Nano-CL-20/2,4,6-trinitrotoluene (TNT) cocrystal explosives were obtained by mechanical ball milling with 0.38 mm grinding beads [39]. A series of nanosized CL-20-based energetic cocrystals were obtained by the application of the electron spray deposition [40]. Liu *et al.*, [41] prepared CL-20/DNDAP cocrystals via an efficient self-assembly in slightly soluble-medium. By the same method, CL-20 and HMX nanocrystals were also obtained [42]. In addition, there are some improved new methods. For example, when prepared pure CL-20/HMX crystal, solvent evaporated from a saturated solution of the stoichiometric mixture in the presence of a high boiling anti-solvent [31]. Li *et al.*, [43] developed a novel method, called, micro channel-confined crystallization strategy, by which CL-20/HMX cocrystal with desired shape and size was prepared.

Cocrystals of CL-20 with RDX

The intermolecular interactions vary. By cocrystallizing energetic molecules with energetic or non-energetic ones, which give rise to the variations of molecular stacking, property and performance, can be modified in the directions of desirable properties for practical applications.

The cage structure of CL-20 contains two five member rings (FMRs) which possesses alternating carbon and nitrogen atoms, while the base (bottom portion) form a boat shaped 6-membered ring (SMRs) in its skeleton. The ring strain possessed by CL-20 makes it special and more energetic among the other cyclic nitroamines (viz. RDX and HMX). Viswanath *et al.*, studied CL-20.RDX cocrystal [44].

CL-20 being highly energetic among the other nitramines has also high positive heat of formation value and it is a green energetic material employed as solid propellant [45-47]. However, it has some drawbacks that it suffers basically from mechanical sensitivity and cost of synthesis. However, cocrystallization of CL-20 with other suitable HEMs and

LEMs is considered as the best crystal engineering technique to reduce its sensitivity [46,48-50] because it masks crystal defects which in turn are responsible for mechanical sensitivity.

The reported results, indicate that CL-20/RDX cocrystals are usually formed in ratios of 1:1 [44] and 1:2 [51] via EM and GM methods, which was confirmed on the basis of spectral and other analytical techniques. The driving force for the formation of CL-20/RDX cocrystals is C−H···O hydrogen bonds occurring between -NO_2 and -CH_2 moieties. The particles obtained by GM method are near-spherical and of uniform size [51] and the other cocrystal morphology clearly shows the sharpness of CL-20 crystal edges being masked and distortion in the orthorhombic structure happens [45]. New crystal phases were presented in the XRD pattern of CL-20/RDX cocrystal. However, the authors comment that single crystal data are needed to be further studied to confirm the refined crystal structure.

RDX

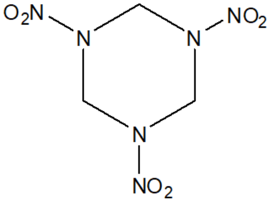

Hang *et al.,* considered CL-20/RDX cocrystal within the constraints of molecular dynamics approach [52]. They have chosen ε-CL-20 to establish the cocrystal model and investigated its properties, because among the four polymorphs (α-, β-, λ-, ε-) of CL-20, ε-CL-20 has the highest energy density, best detonation performance and seems the most promising polymorph [52].

In the study, CL-20/RDX cocrystal models possessing different molar ratios were established by the substitution method and molecular dynamics (MD) simulation method was applied to investigate the influences of molar ratios on mechanical properties, stabilities and detonation performance of cocrystal explosives. In the work, the crystal parameters, structures, binding energies, mechanical properties and some detonation parameters of different cocrystal explosives were got and compared [52]. The results obtained have illustrated that the molar ratio has a direct influence on properties of cocrystal explosive and each of the cocrystal model shows different mechanical properties, binding energies and detonation parameters. The results have revealed that the mechanical properties of CL-20/RDX cocrystal explosive can be effectively improved and the cocrystal model with molar ratio in 1:1 has the best mechanical properties. Additionally, it has the highest binding energy, so that the stability and compatibility is the best. In this article, the molar ratios of CL-20 and RDX (CL-20:RDX) was 10:1, 9:1, 8:1, 7:1, 6:1, 5:1, 4:1, 3:1, 2:1, 1:1, respectively, so that in total 10 kinds of different cocrystal explosives have been investigated. The cocrystal model was established by random substituting method, namely, RDX molecules were used to replace the CL-20 molecules randomly. During the MD simulations conducted, the total number of molecules, volume and temperature were constant. The mechanical properties, stabilities and detonation performance of different cocrystal explosives were got by molecular dynamics (MD) simulation method. The detonation parameters show that the cocrystal explosive has better detonation performance than RDX. The cocrystal explosive with molar ratio in 1:1 has the best mechanical properties, highest binding energy and excellent energy density and detonation performance, hence the authors suggest that it is quite promising and can satisfy the requirements of high energy density compounds (HEDC).

This paper could offer some theoretical instructions and novel insights for the designing of CL-20 cocrystal explosive [52]. The major findings and results were summarized by the authors as follows:

1. The mechanical properties of cocrystal models could be improved owing to the adding of RDX. For the cocrystal explosive with molar ratio in 1:1, the values of tensile modulus, shear modulus and bulk modulus were the least, while Cauchy pressure was the highest, thus implying that the cocrystal model had the best mechanical properties.

2. The binding energies were in the order of 1:1 > 2:1 > 3:1 > 4:1 > 5:1 > 6:1 > 7:1 > 8:1 > 9:1 > 10:1, namely, the compatibility and stability of cocrystal model with molar ratio in 1:1 was the best. Besides, it also meant that CL-20 preferred cocrystalizing with RDX at 1:1 molar ratio.

3. Compared with raw ε-CL-20, the density, oxygen balance (OB), and detonation parameters of cocrystal model decreased gradually, i.e., the energy density and power would be weakened, while the values of detonation parameters were still higher than that of RDX, so the cocrystal explosive had excellent detonation performance.

Namely, the CL-20/RDX cocrystal model with molar ratio in 1:1 had the best mechanical properties, highest binding energy and excellent detonation performance. Therefore, the authors remark that it is worth more further research and experimental tests.

Molecular dynamics is used widely in research on cocrystal explosives [53]. The material models can refer to perfect, defected, and PBX explosives. In such studies, external stimuli such as high temperature, electric field and shock can be considered. Research in the field is currently focused on design and synthesis, structure and properties, the reaction mechanism of decomposition, and sensitivity reduction. Overall, molecular dynamics simulation results provide detailed micro-level information for in-depth understanding of the structure and properties of cocrystal energetic materials [53].

In the work of Wang *et al.*, [54] molecular dynamics simulations of CL-20/RDX cocrystal at different temperatures (200K, 298K, 400K) have been performed. The simulation results were analyzed by radial distribution function (RDF), Hirshfeld surface analysis, and growth simulation. The results show that the CL-20/RDX cocrystal g(r) peak values of O…H at 200K, 298K, and 400K were 1.55, 1.76, and 2.00, respectively. As the temperature of the cocrystal decreases, the hydrogen bonding interaction strengthens. On the other hand, the g(r) peak value of the N-N bond was higher than that of the pure component CL-20, which indicates that the cocrystal enhanced the strength of the N-N bond and therefore reduced the sensitivity of CL-20. At the same temperature, the g(r) value of the N...N bond is lower than N...O, thus CL-20 decomposition starts from the N-N bond. Hirshfeld surface analysis has showed that the O...H contact contribution to the Hirshfeld surface area was 38.2%, which accounted for the largest proportion of interactions, and the de+di value was the smallest. Thus, the interaction distance was the shortest, indicating that the driving force of CL-20/RDX cocrystal formation was derived from hydrogen bonding. The strong interaction of the cocrystal formation should be mainly generated at the nitro group. Also, the hydrogen bond force of the central molecule CL-20 as a hydrogen bond donor is greater than that of a hydrogen bond acceptor. The simulated morphology is long columnar, which is similar to the experimentally prepared morphology, and its rounded shape provides certain advantages in terms of sensitivity [54].

Cocrystals of CL-20 with HMX

A typical new energetic material, CL-20/HMX co-crystal (energetic/energetic type) has been discovered to ameliorate some properties of HMX and CL-20. It is a very promising explosive owing to its high energy (9484 m/s) and low mechanical sensitivity (similar to β-HMX) [36,55-57]. Notably, CL-20/HMX co-crystal has a unique crystal structure formed by orderly arrangement of CL-20 and HMX molecules.

The prepared CL-20/HMX cocrystals possessing high performances and good sensitivity, showed much better overall properties than CL-20/RDX cocrystals [55]. The first cocrystal of CL-20/HMX at a molar ratio of 2:1 had been prepared in 2012 by Matzger [55]. The cocrystals were well characterized by spectroscopic, thermo analytical tools, X-ray diffraction studies, and microscopic techniques. Also a correlation of percentage of cocrystal formation with evaporation rate has been obtained through quantitative analysis by using Raman spectrometry [55]. Later on, much work has been done on CL-20/HMX cocrystals as the most promising high energy combination. A pressure-induced effect of CL-20/HMX cocrystal has been found by DFT technology, [56] indicating that CL-20 plays a dominant role in the electronic structure of this cocrystal. In addition, analysis of the mechanical properties of the CL-20/HMX cocrystal also proves its strong anisotropy. However, a detailed study on the cocrystallization mechanism of the CL-20/HMX may be helpful to improve its quality [57]. Therefore, much work has been done on preparation and performance of CL-20/HMX cocrystals, and in the article the reported preparation methods are summarized [56].

HMX

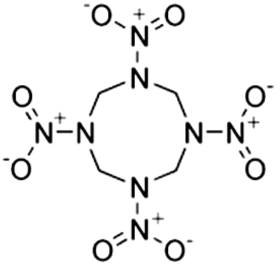

Usually some digital photos assisted with SEM images could be sufficient to determine the morphologies of CL-20-based cocrystals prepared under various experimental conditions, which indicate that the majority of these cocrystals are plate-like in shape. Generally speaking, raw CL-20 particles are spindle-shaped with a size of 30-300 μm, and raw HMX sample particles are usually polyhedral with an average size of 100 μm. [36]. The CL-20/HMX microparticles are composed of many tiny cocrystals, which are plate-shaped. However, the majority of nanosized cocrystal particles show spheroidal morphology. Cocrystals of CL-20/HMX at a 2:1 molar ratio are presented as typical examples with different shapes and sizes depending on the preparation methods. However, it is worth mentioning that the uniformity of cocrystals needs to be further improved for better sensitivity and processability. The density range of CL-20/HMX cocrystals obtained by different preparation methods is 1.95-1.96 g·cm^{-3}.

In the work of Sun *et al.,* the proposed kinetic model was evaluated based on the non-isothermal DSC data by using a non-linear optimization method, which was identified as a complicated reaction comprising two parallel autocatalytic paths. The contribution of the two reaction paths was revealed to vary depending on the heating rate [58]. The thermal hazard simulation has indicated (the data based on the kinetic model) that the temperature when the occurrence of thermal decomposition after 24 hours (Td,24) of CL-20/HMX co-crystal is 151.64 °C, and the critical temperature of 1000th second explosion has been determined as ~196 °C. Besides, the simulation results of self-accelerating decomposition temperature has demonstrated that the package mass of CL-20/HMX co-crystal, rather than the package material, has a remarkable effect on the thermal safety of CL-20/HMX co-crystal [58].

Note that HMX possesses four different kinds of polymorphs (α-, β-, γ-,δ-). Among them, β-HMX is more stable than α-, γ-, and δ-HMX. Previous studies have revealed that crystal defects would directly and greatly affect the properties of EMs. Therefore, the authors also have considered to explore the effects of adulteration crystal defect on properties of HMX. The influences of adulteration crystal defect on sensitivity, energetic properties, and mechanical properties of explosives were explored and investigated by MD method. Some MD simulations were performed with constant pressure and temperature (NPT) ensemble and COMPASS force field in order to accurately predict the properties of different crystal models [58].

Their results have indicated that (the non-isothermal DSC and *in-situ* XRD analysis) CL-20/HMX co-crystal does not experience a phase transformation or melting process before thermal decomposition, which is quite distinct from the behavior of pure CL-20 and HMX crystals. Moreover, according to the isothermal experimental results, the thermal decomposition of CL-20/HMX co-crystal is identified as a typical autocatalytic reaction, so that the heat and gas production rates undergo an acceleration period to approach the maximum value, then followed by a deceleration process.

They observed that the compatibility of non-isothermal DSC results at high heating rates was quite poor, which is probably due to the violation of temperature uniformity in the co-crystal under high heating rates, which has resulted in a micro-explosion with ultra-high exothermic rate. In contrast, the experimental data at lower heating rates can be fitted well by a proper kinetic model, and the thermal decomposition kinetic of CL-20/HMX co-crystal was found to comprise two parallel autocatalytic reactions (paths). The contribution of the two parallel paths was revealed to vary with diverse heating rates because of their different activation energy and heat production. Based on the kinetic model, the simulation results show that the Td,24 of CL-20/HMX co-crystal is 151.64 °C, and the critical temperature of 1000th second explosion is ~196 °C, agreed well with experimental results (199 °C). Besides, according to TCL, it shows that the conversion limit of CL-20/HMX co-crystal at 70 °C will reach 0.1% and 1% after 65 years and 243 years, respectively, indicating good stability of CL-20/HMX co-crystal [58].

In another work of Sun *et al.*, [59] a molecular dynamics (MD) simulation was performed for a ε-CL-20 (2,4,6,8,10,12-hexanitro-2,4,6,8,10,12-hexazisowurtzitane) crystal, a β-HMX (1,3,5,7-tetranitro-1,3,5,7-tetrazocane) crystal, as well as for a ε-CL-20/HMX cocrystal and its composite with the same molar ratio as in the cocrystal using a COMPASS force field with NPT ensemble at different temperatures. The maximum bond length ($L_{\max}$) of the N–NO_2 trigger bond, cohesive energy density (CED) and binding energy (E_{bind}) between HMX and CL-20 molecules as well as elastic properties were calculated. The data have revealed that $L_{\max}$ increases with rising temperature and is found to be in the order of ε-CL-20/HMX cocrystal < CL-20/HMX composite < ε-CL-20 crystal at the same temperature. On the other hand, CED and E_{bind} of the cocrystal decrease with increasing temperature and are all greater than those of the composite at the same temperature. All these findings indicate that the cocrystal is the most insensitive and moreover, its thermal stability is better than that of the composite. Furthermore, the pair correlation function $g(r)$ analysis reveals that hydrogen bonds exist. Also the data revealed that the tensile modulus (E), bulk modulus (K) and shear modulus (G) of the ε-CL-20/HMX cocrystal and the composite are smaller than those of ε-CL-20 and β-HMX crystals which decrease with increasing temperature. However, the K/G values of the cocrystal and the composite are larger than those of the other two crystals, implying that they have better ductility [59].

Ding, *et al.*, [60] studied the thermal decomposition behavior of CL-20/HMX mixed system under different pressure which was investigated by means of high-pressure DSC. Using the thermal decomposition characteristics data of the mixed systems under different pressure some comparisons were done. The thermal decomposition kinetic parameters of CL-20/HMX mixed system (under 0.1 MPa, 1 MPa, 3 MPa pressures) were calculated by means of Ozawa method. The effects of ingredient mixture ratio and pressure on thermal decomposition kinetic parameters were analyzed. The resultant data have revealed that the apparent activation energy of CL-20 in the system increases with pressure and HMX content [60].

Although, usage of high energy, energetic materials (EMs) have been widely applied in the composition of explosives, propellants, and pyrotechnics due to their outstanding combustion efficiency and high energy releasing rate [61,62] potential applications of several nitroamine explosives, such as hexanitrohexaazaisowurtzitane (CL-20), 1,3,5,7-tetranitro-1,3,5,7-tetrazacy-clooctane (HMX) and hexahydro-1,3,5-trinitro-1,3,5-triazine (RDX), [63] are still impeded by their high mechanical sensitivity. To overcome this drawback nowadays, employment of co-crystallization has become popular. As mentioned before, it is a novel technology, which depends on noncovalent interactions including hydrogen bonding, [64] van der Waals forces and π-π stacking [65-67] to efficiently combine independent molecule components.

In the work of Zang *et al.*, [68] nanocrystals of raw ε-CL-20 (37.3 g) and β-HMX (12.6 g) with molar ratio of 2 : 1 were produced by mechanical grinding in water in order to decrease the particle size further and obtain sufficient dispersion and blending of these two explosives, which was followed by centrifugation and freeze drying [68]. For the structure determination of the CL-20/HMX co-crystal, a single crystal was prepared by the interfacial self-assembly strategy in pure H_2O for 4 hours. It was used for the structure determination by single-crystal X-ray diffraction (SCXRD). The quasi-static compression method was employed to evaluate the coherence strength of the as-prepared CL-20/HMX co-crystal [68].

The CL-20/HMX co-crystal (after hydrothermal treatment) exhibited a uniform polyhedral morphology of about 20 μm with a narrow particle size distribution in a reactor. To further explore the CL-20/HMX co-crystal obtained, the size distribution was determined. The results revealed that the CL-20/HMX co-crystals were characterized by a narrow size distribution (19.1 μm) than the individual components, which is consistent with the SEM results.

As outline in their work, CL-20/HMX co-crystals with high purity, uniform morphology, well-proportioned size distribution, compact internal structure and reduced sensitivity were fabricated by a solvent-induced self-assembling approach using corresponding nanoparticles as the basic units. It is worth mentioning that the strategy of interfacial self-assembly is a novel, facile and general method for the fabrication the CL-20/HMX co-crystal. They proposed a mechanism for the assembly of CL-20/HMX cocrystal, and also studied the assembly kinetics of CL-20/HMX co-crystal.

The work is also interesting because of the fact that an interfacial self-assembly strategy was reported for the first time as a novel route to fabricate CL-20/HMX energetic co-crystals. The formation processes were investigated at a particle level, which revealed that they are significantly different from the processes of traditional solvent/non-solvent crystallization occurring at a molecular level. The obtained CL-20/HMX co-crystals, as mentioned, possessed uniform morphology, well-proportioned size distribution, high density, few impurities or defects, characteristic thermal performance and improved safety performance as well. The proposed method in this study was found to be facile, general and environmentally friendly. They claimed that the method can be influenced very slightly by the mass and heat transfer, facilitating its scale-up.

In the study of Zhao *et al.*, [58] the kinetic model was evaluated based on the non-isothermal DSC data and by using non-linear optimization method. The data indicated that a complicated reaction involving two parallel autocatalytic paths occurs, and the contribution of the two reaction paths vary depending on the heating rate. Based on the kinetic model, the thermal hazard simulation indicates that the temperature when the occurrence of thermal decomposition after 24 hours (Td,24) of CL-20/HMX co-crystal is 151.64 °C. The critical temperature of 1000th second explosion is determined as ~196 °C. Besides, the simulation results of self-accelerating decomposition temperature demonstrate that the package mass of CL-20/HMX co-crystal, rather than the package material, has a remarkable effect on the thermal safety of CL-20/HMX co-crystal. To obtain CL-20/HMX co-crystal by using ε-CL-20 and β-HMX as raw materials, a "solvent-media recrystallization" method was employed. The non-isothermal DSC experiments were measured using about 0.8-1.2 mg sample and the temperature range which was set from 30 °C to 280 °C at the heating rate of 0.2, 0.4, 0.6, 0.8, 1, 2, 5, 10 °C/min. On the other hand, the isothermal DSC experiments were carried out in which the isothermal temperature set as 232 °C and 240 °C, respectively. During the DSC experiments pure nitrogen (99.999%) was used as protective carrier gas with a flow rate of 30 ml min^{-1}.

In order to investigate the thermal decomposition behavior of CL-20/HMX co-crystal, the non-isothermal DSC analysis was employed. It was observed that CL-20/HMX co-crystal exhibited only an exothermal peak at heating rates of 1 and 10°K/min, but no endothermic process could be observed. This indicates that CL-20/HMX co-crystal did not undergo a phase transformation or melting process before thermal decomposition. To verify this, the authors performed *in-situ* XRD experiment to examine the crystal stability of CL-20/HMX co-crystal. In order to determine the reaction type of decomposition of CL-20/HMX co-crystal, they performed non-isothermal DSC at several heating rates to evaluate the thermal kinetic parameters. Since CL-20/HMX co-crystal exhibits only one exothermic peak, they have concluded that the parallel paths are coupled during the thermal decomposition [58].

In order to evaluate the thermal stability or storage aging life of a substance, *time to conversion limit (TCL)* was exploited. Also self accelerating decomposition temperature (SADT) was investigated.

As an outline, in this study, the thermal decomposition behavior of CL-20/HMX co-crystal was carefully investigated by DSC, *in-situ* XRD, and isothermal accelerating rate calorimeter (ARC) analysis. The kinetic model of the thermal decomposition of CL-20/HMX co-crystal was successfully created for the first time, and to predict the thermal hazard under different conditions, the kinetic-based simulation was performed [58].

Ghosh *et al.*, described a new preparation method for CL-20/HMX (2:1) co-crystal and supplied structural data and thermo kinetic analysis [31]. The employed solvent evaporation technique yielded pure co-crystals from a saturated solution of the stoichiometric mixture in the presence of a high boiling anti solvent (comparatively a very efficient and cheaper method). The obtained co-crystals were well characterized by spectroscopic, and thermo analytical tools, as well as the X-ray diffraction and microscopic techniques. A correlation of percentage co-crystal formation with evaporation rate has been obtained through quantitative analysis using Raman spectrometry. Evaporation rate of <1 ml/min consistently produced pure co-crystal confirmed by Raman and powder-XRD analysis. The thermo kinetic analysis suggests that the co-crystal to be more stable than CL-20 with energy of activation of 65 kcal/mol, higher than CL-20 but inferior to HMX. Enhanced insensitivity towards friction and impact forces and higher measured velocity of detonation all indicate the improved performance on incorporation into high explosive formulations.

On the other hand, the structural analysis revealed propagating non bonding interactions contributing towards lattice built-up and platelet morphology of the co-crystal. On the other hand, organic additives used showed little control over the alteration of morphology. A detailed analysis of Raman spectra along with mode assignments using a computational method helped to understand the solid phase vibrational modes and thus supporting the observed molecular conformations in the lattice. The characteristics obtained with friction and impact insensitivity figures of 300 N and $h_{50\%}$= 48 cm, respectively indicate the enhanced insensitivity. The observation that the velocity of detonation is well above HMX, endorse the co-crystal to be a better candidate for future insensitive munitions (IMs) [31].

In order to enhance the understanding of the mechanism cocrystal formation, the formation process of CL-20/HMX cocrystal was investigated by Sun *et al.* The research was based on the XRD qualitative/quantitative analysis and using the methods of SEM images in anhydrous acetone, acetone/H_2O solvent admixture and slightly-soluble-medium transition experiment [57]. They have found that the formation process of CL-20/HMX cocrystal experiences significant phase transition from CL-20 and HMX separated precipitations to CL-20/HMX cocrystal in acetone solvent, and also in slightly-soluble-medium. The solvent media and the presence of tiny active secondary nuclei seemed to be necessary in the phase transition process.

It has been found that the formation of CL-20/HMX cocrystal experiences a significant coformers converting process from separated precipitation to cocrystal in acetone solvent. Specifically, β-CL-20 and β-HMX precipitate in anhydrous acetone, while β-HMX, β-CL-20 and α-CL-20 precipitate in acetone/H_2O solvent pair [57]. They verified this process by performing a slightly-soluble-medium transition experiment in ethanol solvent. Accordingly, solvent media and tiny active secondary nuclei are identified as having the key roles in phase transition. The conversion from tiny active nuclei (produced by secondary nucleation) to cocrystal with heterogeneous molecules in solvent is thermodynamically allowed. All the three crystal phases (β-, α-, ε-) of CL-20 together with β-HMX can be converted to cocrystal. Based on this, they found the solvent evaporation is a long and useless process. Cocrystal, they have reported, can be obtained more efficiently by the slightly-soluble-medium transition experiment. The authors believe that some environmentally slightly soluble solvents can play an unexpected role in cocrystal preparation. Also the feasibility of slightly-soluble-medium transition method is verified by CL-20/TNT, BTF/TNT and BTF/TNB cocrystals [57].

Ultrafine cocrystal explosives attract scholarly attention in order to reduce mechanical sensitivity. Because, it is known that mechanical sensitivity can be reduced by decreasing particle size of explosives [69,70]. Ultrafine explosive particles have some advantages over larger ones in improving burning rate of solid propellants [71-73].

In the work of An *et al.*, [36] the spray drying method was used to prepare cocrystals of hexanitrohexaazaisowurtzitane (CL-20) and cyclotetramethylene tetranitramine (HMX) in 2/1 molar ratio. Raw materials and cocrystals were characterized by using scanning electron microscopy, X-ray diffraction, differential scanning calorimetry, Raman spectroscopy, and Fourier transform-infrared spectroscopy. Impact and friction sensitivity of cocrystals were tested and analyzed. The XRD and DSC patterns revealed that cocrystal explosive was not the intimate mixture of CL-20/HMX. The results showed that, after preparation by spray drying method, microparticles were spherical in shape and had the size of 0.5–5 μm. Particles formed aggregates of numerous tiny plate-like cocrystals, whereas CL-20/HMX cocrystals had thicknesses of below 100 nm. Cocrystals were formed by C–H· · ·O bonding between $–NO_2$ groups of CL-20 and $–CH_2–$ units of HMX. The nanococrystal explosives exhibited drop height of 47.3 cm, and friction demonstrated explosion probability of 64%. These tiny cocrystals do not disperse individually but rather agglomerate into microparticles ranging from 0.5 μm to 5 μm in size. Peak decomposition temperature of the cocrystal explosives is 246.98 °C, which is 3.86 °C lower than that of CL-20. Compared with that of HMX, the nanococrystals manifested significant decrease in impact and friction sensitivities. The drop height increased by 141%, and friction probability reduced by 20%. Nano-CL-20/HMX cocrystal explosive exhibits insensitivity to mechanical action. As compared with raw HMX, the cocrystals possessed significantly reduced mechanical sensitivity [36].

Great research efforts have been spent in order to tailor and improve the properties of EMs by adjusting or modifying substance compositions, controlling material morphology [74], reducing particle size [75], and synthesizing new materials [76]. Through the years, it has been observed in the field of material science that co-crystals have great potentials in various important applications by adjusting their crystal structure at the molecular level [77-83]. Note that by means of co-crystallization technology, the physico-chemical properties of two independent components can be efficiently combined and produced a modified material in the direction of amelioration of the properties.

Gao *et al.,* performed a facile, large-scale synthesis of an energetic nanoscale cocrystal composed of a 2:1 molar ratio of CL-20 and HMX via the ultrasonic spray-assisted electrostatic adsorption (USEA) method [84]. The product mean particle size was 50 nm, and the particle size distribution was relatively in narrow range. The cocrystal produced was stable because of a number of C-H hydrogen bonds, each involving oxygen atoms of the nitro group(s). The density of the nano-sized CL-20/HMX co-crystal was 1.945g cm^{-3} and high to 2.006 g cm^{-3} at 0 °K. Its detonation velocity was 9480 m s^{-1}, which was higher than that of pure HMX explosive and comparable with that of pure CL-20. The cocrystal CL-20/HMX exhibited high energy-release efficiency and a unique exothermic peak at 243.5 °C. The peak shifts left by 40 °C compared to that of pure

HMX. This strategy not only combined the advantages of cocrystals and nano effects but also opens up new perspectives and advances in the development of the science and technology of organic cocrystal materials. The method is claimed that it may be employed in industrial production on a large scale preparation of high-performance materials with excellent properties [84].

There is great interest in the field of explosives for reducing initiation sensitivity of energetic materials, particularly of those based on more powerful and generally more sensitive high explosives (HEs) including 2,4,6,8,10,12-hexanitro-2,4,6,8,10,12-hexaazaisowurtzitane (CL-20) and 1,3,5,7-tetranitro-1,3,5,7-tetrazocine (HMX) [85-89]. As accidental detonations of them can result in loss of lives and tremendous cost. One of the strategies that is currently pursued to retain the performance of these explosives while significantly reducing their sensitivity is to employ their cocrystals in formulations, [90-91] because cocrystals can have distinct properties compared to the corresponding coformer crystals.

The 2CL-20 • HMX cocrystal was first produced by Bolton *et al.,* by a solution precipitation route [55] and has since been made by solvent drop grinding using resonant acoustic mixing [92]. Note that the solvent drop grinding is a commonly used variation to the solid-state grinding employed in mechanical cocrystal formation [93]. The addition of a little amount of suitable solvent can facilitate the formation of cocrystals [94]. However, in the case of these methods impurities, typically in the form of coformer crystals, are commonly observed in the final product. Furthermore, the 2CL 20 • HMX cocrystal prepared by these techniques often has a relatively large particle size with undesirable plate-like morphology.

Qiu *et al.*, in their work prepared energetic nanoscale 2CL-20 • HMX, a cocrystal of CL-20 and HMX (at a 2:1 molar ratio) by using a novel method (bead milling) and an aqueous suspension of ε-CL-20 and β-HMX [39]. Conversion of the coformers to the cocrystal form was monitored by powder X-ray diffraction (XRD) and scanning electron microscopy (SEM) analysis of specimens sampled at various milling times. They found that complete conversion to the cocrystal form was achieved after the period of 60 minutes of milling. Rounded 2CL-20 • HMX cocrystal particles with a mean size below 200 nm were produced. A mechanism for the conversion of the coformers to the cocrystalline form is postulated based on the experimental results.

Compared to other processes, production of 2CL-20 • HMX cocrystal by bead milling has some distinct features.

(1) The process is shown to completely convert the coformer crystals to the cocrystalline form. This is important as impurities can affect the properties of HEs, especially the sensitivities dramatically.

(2) Extremely small cocrystal particles with rounded morphology are attained. These features are expected to reduce the shock sensitivity of the energetic cocrystal.

(3) The conversion process takes place in aqueous media and the obtained nanoscale cocrystal particles are in a suspension, which make the aqueous bead milling process inherently safe and uniquely suitable for the production of HE crystals in terms of process safety.

So, as an inherently safe manufacturing method, the aqueous bead milling process has a great potential in advancing the cocrystal research and applications in the field of energetic materials.

In the work of Han *et al.,* a 2,4,6,8,10,12-hexanitro-2,4,6,8,10,12-hexaazaisowurtzitane (CL-20) /1,3,5,7-tetranitro-1,3,5,7-tetrazacyclooctane (HMX)-isopropanol (IPA) interfacial model was constructed in order to investigate the effect of temperature on cocrystal morphology [95]. A constant volume and temperature molecular dynamics (NVT-MD) simulation was performed on the interfacial model at various temperatures (295–355 K, 20 °K intervals). The surface electrostatic potential (ESP) of the CL-20/HMX cocrystal structure and IPA molecule were studied at the level of B3LYP/ 6–311++G (d,p). The surface energies, polarities, adsorption energy, mass density distribution, radial distribution function (RDF), mean square displacement (MSD) and relative changes of attachment energy all were analyzed. The results revealed that polarities of (1 0 0) and (0 1 1) cocrystal surfaces may be more negative and affected by IPA solvent. The adsorption energy per area indicates that growth of the (1 0 –2) face in IPA conditions may be more limited, while the (1 0 0) face tends to grow more freely. The MSD and diffusion coefficient (D) analyses have demonstrated that IPA molecules gather more easily on the cocrystal surface at lower temperatures, and hence have a larger effect on the growth of cocrystal faces. The RDF analysis shows that, with the increasing of temperature, the strength of hydrogen bond interactions between cocrystal and solvent becomes stronger, being highest at 335 °K for the (1 0 0) and (0 1 1) interfacial models. The results of relative changes of modified attachment energy indicate that (1 0 0) and

(0 1 1) faces tend to be larger than the other faces. Moreover, the predicted morphologies (at 295 and 355 °K) which are consistent with experimental values, proves that the CL-20/HMX-IPA interfacial model is a reasonable one for this study [95].

As an outline, in the work the CL-20/HMX-IPA interfacial model was built to study the effect of solvent on the growth morphology from gaining insights into solvent behaviors at different temperatures. Quantum chemistry calculations for the CL-20/HMX cocrystal framework and IPA molecule were also performed. The authors have pointed out that the following main conclusions can be drawn from their investigation:

(1) The polarities of (1 0 0) and (0 1 1) faces may be more negative because there are more exposed nitro groups (HMX) than other faces. Therefore, the latter three faces may be less affected by the IPA layer and will grow more freely in the solvent environment, and hence be less morphologically important.

(2) The orders of adsorption energy per unit area (Ea, ave) at different temperatures are the same: (1 0–2) > (1 1 0) > (11 1) > (0 1 1) > (1 0 0), meaning that the interaction between the solvent and the (1 0–2) face is strong while that with the (1 0 0) face is weak. However, the Ea, ave values of all situations are close to each other.

(3) The MSD and diffusion coefficient of solvent molecules shows that the lower temperature is beneficial to the interaction between cocrystal surfaces and solvent. RDF analysis shows the existence of strong hydrogen bonds for (1 0 0) and (0 1 1) interfacial models at 335 K, and, therefore, a more obvious inhibition effect on crystal growth.

(4) The relative changes in modified attachment energy show that cocrystal surfaces (1 0 0) and (0 1 1) will change less at 295 K compared with those at high temperatures, consistent with the total facet area variations. The predicted morphology of the CL-20/HMX cocrystal is in accordance with the experimental shape, indicating the applicability of interfacial model for this study.

Although this work may provide some theoretical guidelines for the preparation of cocrystal explosives, such as the selection of solvent, it must be kept in mind that cocrystal morphology can be affected by many factors, and the authors believed that more work should be done to explain influential factors on the morphology mechanism in the future.

In the work of Jia *et al.*, 2HNIW.HMX cocrystal is considered and the influence of temperature and solvent on the solid–liquid ternary phase diagrams of it has been investigated [96]. The ternary phase diagrams were constructed for the 2HNIW.HMX cocrystal in acetonitrile and ethyl acetate at 15 °C and 25 °C. HMX and HNIW showed inconsistent dissolution behavior and congruent dissolution behavior in acetonitrile and ethyl acetate, respectively. On the other hand, in the HMX–HNIW–acetonitrile ternary system, the 2HNIW.HMX cocrystal has a narrow thermodynamically stable region at both temperatures. Whereas, the cocrystal exhibits a wider thermodynamically stable region in the HMX–HNIW– ethyl acetate system. The results have shown that the choice of solvent has a crucial influence on the dissolution behavior of the cocrystal and the size and position of each region in the phase diagram, while the temperature has no apparent effect on the overall appearance of the phase diagram. Therefore, by properly selecting the ratios, the 2HNIW.HMX cocrystal could be prepared by the isothermal slurry conversion crystallization method [96].

It is now being understood that cocrystals with the required characteristics (such as decreased impact sensitivity of HNIW allows its applicability in various fields) possibly play an important role in future weaponry, propellant and HEMs. Also note that decreasing the impact sensitivity of HNIW may help the manufacturers to take due care at the time of synthesis.

Cocrystallization can change the internal composition and crystal type of EMs without destroying the chemical structure of the original materials. Thus, it has been the focus of tremendous effort in order to modify their performances efficiently. These properties of explosives to be modified (such as higher density, better explosive performance, lower sensitivity, and better stability) could be acquired through cocrystals formation with other EMs or non-energetic materials.

Note that 2HNIW·HMX co-crystals are crystals composed of HNIW and HMX molecule are combined with noncovalent bonds in a lattice at a 2:1 ratio. In the study of Zhang *et al.*, the 2HNIW·HMX co-crystals were synthesized and characterized by XRD, Raman spectra, DSC, and HPLC [97]. The collected data have revealed that the standard enthalpy of formation of 2HNIW·HMX cocrystals is 861.9 ± 18.6 $kJ \cdot mol^{-1}$ under the direction of a designed thermo chemical cycle with a Calvet micro calorimeter. The thermal decomposition behavior of 2HNIW·HMX co-crystals was studied under the non-isothermal condition with DSC. The apparent activation energy (E) of the decomposition is 332.23 $kJ \cdot mol^{-1}$ by Kissinger method, 324.10 $kJ \cdot mol^{-1}$ by Ozawa method, 314.06 ± 4.26 $kJ \cdot mol^{-1}$ by Friedman-Reich-Levi method, respectively. Whereas a smaller value; 306.81 ± 3.12 $kJ \cdot mol^{-1}$ was obtained by NL-INT-SY3 method. The pre-exponential factor ($\log A/s^{-1}$) is 29.33 ± 0.33 via compensation effect. A continuous Cp mode of

Micro-DSC III was used to determine the specific heat capacity (Cp,m) of the target co-crystals from 283.15 to 333.15 K, and the Cp,m is 1114.04 ± 10.92 $J\cdot mol^{-1}\cdot K^{-1}$ at 298.15 K.

The thermal decomposition parameters (Te0 = 498.82 K, Tp0 = 505.03 K, and Tb = 505.75 ± 0.12 °K) of 2HNIW·HMX co-crystals have been acquired. The entropy of activation ($\Delta S^{\ddagger}$), enthalpy of activation ($\Delta H^{\ddagger}$), and Gibbs free energy of activation ($\Delta G^{\ddagger}$) of the exothermic decomposition stage are obtained as 303.88 ± 6.32 $J\cdot mol^{-1}\cdot K^{-1}$, 302.64 ± 3.12 $kJ\cdot mol^{-1}$, and 149.17 ± 3.86 $kJ\cdot mol^{-1}$. Note that these parameters can contribute to the understanding the thermal property of 2HNIW·HMX cocrystals. The specific heat capacity of 2HNIW·HMX co-crystals is $Cp,m/(J\cdot mol^{-1}\cdot K^{-1}) = -4.35692 \times 10^3 + 4.32914 \times 10^1(T/K) - 1.13468 \times 10^{-1}(T/K)^2 + 1.00000 \times 10^{-4}(T/K)^3$ from 283.15 to 333.15 °K and the Cp,m is 1114.04 ± 10.92 $J\cdot mol^{-1}\cdot K^{-1}$ at 298.15 °K. In addition, also the enthalpy change and entropy change of 2HNIW·HMX co-crystals within 283.15 and 333.15 °K, (taking 298.15 °K) have been obtained. These results obtained can provide valuable information for both the theory and applications of co-crystalline materials.

In the work of Zhang *et al.*, co-crystal of (HNIW).(HMX) in a 2:1 molar ratio was prepared by a solvent/non-solvent method, and then the co-crystal has been characterized by several methods [98]. The enthalpies of dissolution of 2HNIW·HMX co-crystal in N,N-dimethylformamide at different temperatures have been measured by using a DC08-1 Calvet micro calorimeter under standard atmospheric pressure, and it is indicated that the dissolutions are exothermic process. The empirical formulae for the calculation of the molar enthalpy ($D_{diss}H$) of dissolution, relative partial molar enthalpy ($D_{diss}H_{partial}$), relative apparent molar enthalpy ($D_{diss}H_{apparent}$), and enthalpy of dilution ($D_{dil}H_{1;2}$) at 298.15 K are all obtained. Additionally, the differential enthalpies ($D_{dif}H$) and kinetic equations describing the dissolution process at different temperatures are deduced. Furthermore, the apparent activation energy E = 10.54 ± 0.22 kJ mol^{-1} and pre-exponential constant A = 0.34 ± 0.03 s^{-1} of 2HNIW.HMX co-crystal are obtained. The standard molar Gibbs free energy of activation at different temperatures are found to be 86.44 ± 0.02 kJ mol^{-1} (298.15 K), 88.02 ± 0.03 kJ mol^{-1} (303.15 K), 89.61 ± 0.01 kJ mol^{-1} (308.15 K), 91.18 ± 0.01 kJ mol^{-1} (313.15 K), and 92.75 ± 0.02 kJ mol^{-1} (318.15 K), respectively. Whereas, the standard molar entropy of activation and standard molar enthalpy of activation values are - 262.55 ± 0.72 J mol^{-1} K^{-1} and 7.98 ± 0.22 kJ mol^{-1}, respectively.

The main points in the work are

1. Acetonitrile and distilled water are chosen as solvent and non-solvent to prepare the 2HNIW.HMX cocrystal by S/NS method. To investigate the structure and properties of the co-crystal is characterized by PXRD, FTIR, Raman spectra, DSC, and HPLC.

2. The values of heat effect of 2HNIW·HMX co-crystal dissolving in DMF at different temperatures are measured by a DC08-1 Calvet micro calorimeter, and the dissolutions are found to be exothermic processes. The empirical formulae ($\Delta_{diss}H$, $\Delta_{diss}H_{apparent}$, $\Delta_{diss}H_{partial}$, and $\Delta_{dil}H_{1;2}$) describing the dissolution properties of 2HNIW.HMX at 298.15 °K are obtained according to the experimental data. In addition, the values of $\Delta_{dif}H$ at different temperatures are acquired.

3. The kinetic equations for the dissolution processes of 2HNIW·HMX co-crystal at different temperatures have been obtained as follows:

$$d\alpha/dt = 10^{-2:32}(1 - a)^{1:04} \qquad (T = 298:15\ °K)$$

$$da/dt = 10^{-2:29}(1 - a)^{1:09} \qquad (T = 303:15\ °K)$$

$$da/dt = 10^{-2:26}(1 - a)^{1:16} \qquad (T = 308:15\ °K)$$

$$da/dt = 10^{-2:23}(1 - a)^{1:25} \qquad (T = 313:15\ °K)$$

$$da/dt = 10^{-2:21}(1 - a)^{1:28} \qquad (T = 318:15\ °K)$$

4. The apparent activation energy E and the preexponential factor A are obtained as 10.54 ± 0.22 kJ mol^{-1} and 0.34 ± 0.03 s^{-1}, respectively. The activation values of ΔG, ΔS and ΔH at different temperatures, are obtained by calculation.

Song, *et al.*, gives a good account of the thermal decomposition and various properties of some C20-based cocrystals [51]. The thermal decomposition temperature of CL-20/RDX cocrystal has found to be completely different from that of raw ε-CL-20, RDX, and it is reduced. It shows that the CL-20/RDX ECCs has weak intermolecular forces, which leads to a reduced thermal stability [51]. When CL-20 is combined with HMX, a more attractive cocrystal with reduced sensitivity can be obtained. In the work various the DSC curves of CL-20/HMX cocrystal explosive, and their experimental data are provided. It has been shown that the thermal properties of CL-20/HMX cocrystals make them more chemically stable. Several cocrystals exhibit sharp decomposition peaks at around 247 °C, slightly higher than the other cocrystals due to a smaller cocrystal particle size. On the other hand, the CL-20/HMX prepared by RAM has the best thermal stability, showing an exothermic peak at 248.3 °C. In a word, the peak decomposition temperature of CL-20/HMX cocrystals is close to that of CL-20. It is inferred that the decomposition of CL-20 based cocrystals is initiated by collapse of CL-20 molecules.

In addition, due to the strong nonbonding interactions (hydrogen bond and strong van der Waals force) between CL-20 and HMX molecules, the released heat from their cocrystals is significantly higher than that of the physical mixture with the same molar ratio. In order to make the energy release of EMs more efficient, transition metal compounds are usually added as combustion catalysts.

It is shown that CL-20/HMX ECCs are less sensitive to the same external impact and friction stimulation in comparison with the pristine ε-CL-20. For example, compared with that of β-HMX, nano-cocrystals manifested significant decrease in impact and friction sensitivities, with drop height increased by 141.3%, and friction probability reduced by 20%.

At the same time, they also carried out some comprehensive analysis based on the morphology and sensitivity data. It has been shown that the mechanical sensitivity of the ECCs largely depends on their shape and particle size. The 2 CL-20/HMX cocrystals with relatively larger particle size and undesirable plate-like morphology have higher sensitivity than the nanospherical counterparts. The authors have explained it believing that it is because of the larger cocrystal particles should have introduced some crystalline defects and have fewer interfaces between particles to absorb and disperse the energy from the external stimuli. The impact sensitivity thereby decreases with the decrease of particle size.

The authors contemplate that, if interfaces of the particles and defects could be ignored, the enhanced intermolecular physical forces of attraction (for example, the hydrogen bonding between CL-20 and HMX molecules) may account for the improved insensitivity. Furthermore, stronger nonbonding interactions may promote heat dissipation through nonradiative heat transfer mechanisms, thereby reducing the generation of hot spots. Thus, tailoring intermolecular interactions by incorporating molecules that can create stronger interactions over those of parent materials may be fruitful to elevate the insensitivity of EMs in terms of detonation performance [51].

The velocity of detonation (VD) of HMX/CL-20 cocrystal is 9480.0 $m \cdot s^{-1}$, which is higher than that of pristine β-HMX, even reaching the level of pristine ε-CL-20. Moreover, the calculated VD of CL-20/HMX crystal was higher than that of HMX but lower than that of CL-20.

For the purpose of achieving insensitive CL-20 based ECCs, plenty of cocrystals have been fabricated with the combination of CL-20 and HMX. In the article there exist a list of those cocrystals. It shows that the composite modified double base propellant with CL-20/HMX cocrystal as the high-energy component has high stability, low mechanical sensitivity, and good combustion performance. However, the authors remark that the stability of CL-20/HMX cocrystals during manufacturing of this propellant cannot be ignored due to presence of polar plasticizers, which partially dissolve cocrystals during curing and storage stages. In order to promote practical applications of CL-20/HMX cocrystals, the thermal decomposition kinetics of the cocrystals has been investigated. The decomposition kinetic parameters of cocrystals have been calculated by using the methods Kissinger and Ozawa [31]. The results have shown that the thermal stability of the CL-20/HMX cocrystal is between those of β-HMX and ε-CL-20. For the purpose of achieving insensitive CL-20 based ECCs, plenty of cocrystals have been fabricated with the combination of CL-20 and HMX. In addition, the isothermal DSC experiments demonstrate that the thermal decomposition of the CL-20/HMX cocrystal is a typical autocatalytic reaction. It has been found that the ultrafine CL-20/HMX cocrystal has better compatibility with common components of solid propellants, such as NG/BTTN, AP, and Al [99].

The Cocrystals of CL-20 with TNT

Jia, *et al.,* investigated the phase behavior of a HNIW·TNT cocrystal system [100]. Firstly, the 1:1 HNIW·TNT cocrystal was successfully prepared by solvent evaporation, solvent/nonsolvent, and isothermal slurry conversion crystallization techniques. Then, the formed cocrystal was comprehensively characterized by powder X-ray diffraction (PXRD), differential scanning calorimetry (DSC), Fourier transform infrared (FTIR) spectroscopy, Raman spectroscopy, and scanning electron microscopy (SEM). The influence of temperature and solvent on the phase behavior of a 2,4,6,8,10,12-hexanitrohexaazaisowurtzitane-2,4,6-trinitrotoluene (HNIW·TNT) cocrystal system has been investigated. To design and operate the cocrystal manufacturing process, a systematic study of cocrystal phase diagrams is essential and necessary [101,102]. The ternary phase diagrams can describe the thermodynamic stability region of the desired cocrystal, depending on the solubilities of the two components in a given solvent [103-105]. It has been found that a similar solubility likely leads to a congruent system; conversely, a large solubility difference is likely to obtain an incongruent system.

Therefore, the solubilities of the two components play an essential role in the size and position of the thermodynamic stability region of the cocrystal. In the work, the ternary phase diagrams for HNIW and TNT in acetonitrile and ethyl acetate have been constructed at 25 and 35 °C, indicating that the cocrystal dissolves incongruently in acetonitrile and congruently in ethyl acetate. The results show that the solubility ratio of the two cocrystal components does not provide a reliable and accurate way to predict whether the phase behavior of the HNIW·TNT cocrystal is congruent or incongruent. The construction of the ternary phase diagram identified the thermodynamic stability regions for the cocrystal. In each phase diagram, a broad thermodynamic stability region of cocrystal exists. The appearance of the phase diagram depends strongly on the choice of solvent, and the temperature has a weak effect on the phase diagram. By proper selection of the ratios, the HNIW·TNT cocrystal has been prepared by an isothermal slurry conversion crystallization method and systematically characterized. Compared with the temperature, the choice of solvent has a more critical influence on the dissolution behavior of cocrystal and the appearance of the phase diagram.

TNT

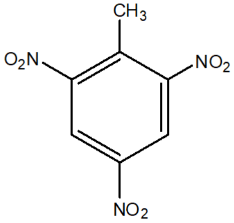

Hu *et al.*, in their work, published in 2020, successfully prepared nano-CL-20/TNT cocrystal explosive by mechanical ball milling with 0.38 mm grinding beads [39]. The high energy level of CL-20 is accompanied by high sensitivity. Previous studies have demonstrated that the characteristic drop height of elemental CL-20 is approximately 10 cm, [106] which severely limits its application in energetic materials. Hence, great effort has been invested in reducing the sensitivity of CL-20 [107-109]. In the work of Hu *et al.*, the micro morphology and particle size of cocrystal explosive were characterized by scanning electron microscopy. The average particle size of nano-CL-20/TNT cocrystal explosive was found to be 119.5 nm and showed a spherical-like micro morphology. The crystal structure of cocrystal explosive was characterized by powder X-ray diffraction, infrared spectroscopy, and Raman spectroscopy. The results show that mechanical ball milling does not change the molecular structure of the raw material, but the sample after ball milling has a new crystal phase, rather than a simple mixing of raw materials. On the other hand, differential scanning calorimetry tests show that nano-CL-20/TNT cocrystal explosive has a higher decomposition temperature and impact sensitivity tests show that the properties of cocrystal explosive are 26 and 21.7 cm higher than those of CL-20 and CL-20/TNT mixture, respectively, which clearly indicates that nano-CL-20/TNT cocrystal explosive has better thermal stability and safety [39].

In order to gain an atomistic-level understanding of the experimental observation that the cocrystal TNT/CL-20 leads to decreased sensitivity, Guo *et al.*, carried out reactive molecular dynamics (RMD) simulations using the ReaxFF reactive force field [110]. They compared the thermal decomposition of the TNT/CL-20 cocrystal with that of pure crystals of TNT and CL-20 and with a simple physical mixture of TNT and CL-20. It has been found that the cocrystal has a lower decomposition rate than CL-20 but higher than TNT, which is consistent with experimental observation. The rupture of the $N–NO_2$ bond dominates the initial steps of CL-20 dissociation followed by ring-breaking reaction. They have found that the formation of carbon clusters arising from TNT (a carbon-rich molecule) plays an important role in the thermal decomposition process, which explains the decrease in sensitivity for the cocrystal. At low temperature and as well as in the early stage of chemical reactions under high temperature, the cocrystal releases energy more slowly than the simple mixture of CL-20–TNT. These results clearly confirm the expectation that co-crystallization is an effective way to decrease the sensitivity of energetic materials while retaining their high performance [110].

Yang *et al.,* published an article on preparation, structure and properties of CL-20/TNT cocrystal [111]. In the work, a novel CL-20/TNT cocrystal explosive was prepared by cocrystallization in solution, and its morphology was characterized by scanning electron microscopy (SEM). Its crystal structure was determined using single crystal X-ray experiment. The results show that the crystal is orthorhombic, having space group Pbca with crystal parameters of a=0.9735(2) nm, b=1.9912(6) nm, c=2.4695(6) nm, $\alpha=\beta=\gamma=90°$, V=4.787 nm^3, and Z=8. The thermal decomposition and impact sensitivity of the product were measured by differential scanning calorimetry (DSC) and sensitivity test, respectively. The results reveal that the exothermic decomposition of CL-20/TNT cocrystal explosive occurs in the temperature range of 180-275°C, and the melting point of TNT significantly increases by about 50°C. Additionally, CL-20/TNT cocrystal has lower impact sensitivity and the results have shown that the impact sensitivity of CL-20 reduces by 87% [111].

In the study of Cao *et al.,*some molecular dynamics (MD) simulations were carried out to investigate the polymer-bonded explosives (PBXs) in which the base explosive was the well-known (CL-20/TNT), that is high energy co-crystal compound, 2,4,6,8,10,12-hexanitro-2,4,6,8,10,12-hexazaisowurtzitane/2,4,6-trinitrotoluene [112]. The polymer binders used were fluorine rubber (F23112311), fluorine resin (F23142314), polyvinyl acetate (PVAc) and polystyrene (PS), respectively. In their article, the binding energies, pair correlation functions (PCFs) and mechanical properties of the PBXs have been reported. According to their theoretical results of binding energies, the compatibility of the PBXs is predicted to be in the order of CL-20/TNT/PVAc >> CL-20/TNT/F23112311 >> CL-20/TNT/PS >> CL-20/TNT/F234 2314.

Also, the binding energies of the PBXs on three crystalline surfaces, namely (100), (001), and (010), of the CL-20/TNT co-crystal were obtained and compared. The orders have been found as CL-20/TNT(100) >> CL-20/TNT(001) >> CL-20/TNT(010) for F23112311, F23142314, and PS, whereas the order is CL-20/TNT(001) >> CL-20/TNT(100) >> CL-20/TNT(010) for PVAc. On the other hand, the PCF analysis reveals that there exist many H-bonds between H and O, F, and N atoms on all three interfaces. Among all H-bonds, N H-bond has the fewest number. For the CL-20/TNT co-crystal, the moduli can be reduced by adding a small amount of the polymer binders but the ductility can be prolonged only by F23112311 and F23142314 [112].

In the process of actual production, storage, transportation and use, explosives are often likely to suffer from external stimuli, especially heat and shock. Under the action of these two common stimuli, the response of cocrystal explosives is of concern. Since, it has been generally accepted fact that the cocrystallization well reconciled the performance of the two components, which is difficult to achieve in a physical mixture system, Li and coworkers investigated CL-20/TNT decomposition under shock [113]. In the wok, the cocrystallization strategy is considered to be an effective means to adjust the various properties of explosives. It has been found in some previous studies that the initial decay steps in pure crystals remain still in the cocrystal. Nevertheless, the underlying mechanism of the effect of the special cocrystal structure on the decomposition process is not clear enough. Their work compares the response processes of a CL-20/TNT cocrystal structure and an amorphous structure under shock waves with different velocities [113]. The CL-20/TNT cocrystal model and amorphous structure model are constructed respectively. The shock waves with velocities of 6-9 km s^{-1} are applied to the two models by multiscale shock technology. The response processes of the two models under different shock waves are simulated. The thermodynamic evolution, reactant decay, product formation, main initial reactions and cluster evolution are analyzed. As a result, it has been found that the amorphous structure is easier to compress than the cocrystal structure, achieving higher stress and temperature and these thermodynamic parameters have a strong correlation. For the amorphous structure, the results reveal that the chemical reaction of the system is more intense, the reactants decay faster, the products are more abundant, and the intermediate products can complete the transformation to stable products earlier. Furthermore, NO_2 is the most important intermediate product, and its quantitative change can directly reflect the reaction process. On the other hand, the amorphous structure seems to be more prone to decomposition reaction, whereas the cocrystal structure is more prone to polymerization reaction. Furthermore, the cluster size in the amorphous structure is smaller and more conducive to decomposition [113].

In the investigation of Wang *et al.*, ultrafine CL-20/TNT cocrystal explosive was prepared by a spray drying method [114]. Thereafter, scanning electron microscopy(SEM) was employed to characterize the particle size and morphology of the crystals. To determine whether the cocrystal explosive was prepared or not techniques of X-ray diffraction(XRD) and differential scanning calorimetry (DSC) were utilized. Furthermore, the impact sensitivity of cocrystal explosive has been tested. The results show that the prepared samples are not the mixture of CL-20 and TNT but rather ultrafine CL-20/TNT cocrystal explosives. The particle size of cocrystal explosives are under 1 μm and they aggregate into many microparticles, which are spherical in shape and range between 1-10 μm in size. The melting point of ultrafine CL-20/TNT cocrystal explosive is 132.32 °C. The thermal decomposition process can be divided into two stages. The peak temperatures of exothermic decomposition for first and second stage are 218.98 °C and 253.15 °C, respectively. The characteristic height of CL-20/TNT cocrystal explosives has been found to be 49.3 cm, which is 36.2 cm higher compared with raw CL-20 explosive [114].

Co-crystallization has splendid advantages or merits for ECs. For example, co-crystallization could strengthen thermal safety, improve mechanical properties, increase energy density, and reduce mechanical sensitivity and so on. In the article, by Hang *et al.*, the CL-20, TNT, HMX, CL-20/TNT, CL-20/HMX and different ternary CL-20/TNT/HMX cocrystal models were established [115]. In this work, the crystal polymorph of CL-20 was chosen as ε-CL-20 because this polymorph was more stable and had better energetic performance than other polymorphs (α-, β-, γ-CL20). In cocrystal models, the molar ratio of different components affects the properties of cocrystal explosives. If the mass percent of high-power component was too much, the cocrystal explosive might have a high crystal density and superior energetic performance. However, the mechanical sensitivity would also be increased. Therefore, too much of a molar ratio of high energy density component would have a positive influence on energetic performance, but a negative effect on safety of cocrystal explosives. On the contrary, if the low power component occupied too much, the cocrystal explosive might present low sensitivity. However, the energy density would be severely weakened at the same time. It was also a negative factor for cocrystal explosives. Therefore, to ensure that the cocrystal explosive has desirable energetic performance and appropriate mechanical sensitivity, the molar ratio of different components should be determined or controlled at a reasonable and proper extent. After establishing the models, molecular dynamics method was selected (the COMPASS force field) to optimize the structures, predict the stability, sensitivity, energetic performance, and mechanical properties of cocrystal models. Note that the force field directly affects the parameters of crystal systems and each force field might be only suitable for limited crystal models. In the work, the binding energy, trigger bond length, trigger bond energy, cohesive energy density, detonation parameters, and mechanical properties of each crystal model were obtained. The influences of co-crystallization and molar ratios on performances of cocrystal explosives were investigated and evaluated. The results show that the CL-20/TNT/HMX cocrystal explosive with a molar ratio of 3:1:2 or 3:1:3 had larger binding energy and better stability, i.e., CL-20/TNT/HMX cocrystal explosive was more likely to be formed with these molar ratios. The cocrystal explosive had shorter maximal trigger bond length, but larger trigger bond energy and cohesive energy density than CL-20. Namely, the cocrystal explosive had lower mechanical sensitivity and better safety than CL-20 and the safety of cocrystal model was effectively improved. On the other hand, the cocrystal model with a molar ratio of 3:1:2 had the best safety. The energetic performance of the cocrystal explosive with a molar ratio of 3:1:1, 3:1:2, or 3:1:3 was found to be the best. These ternary CL-20/TNT/HMX cocrystal models exhibited better and more desirable mechanical properties. Thus, the cocrystal model with molar ratio of 3:1:2 exhibited the most superior properties and was a novel and potential high-energy-density compound. The paper could provide some practical and helpful guidance and theoretical support to better understand co-crystallization mechanisms and design novel energetic cocrystal explosives [115].

Chen and coworkers performed molecular dynamics simulations (MD) (within Discover code) for the purpose of studying the difference of mixing and cocrystallization of TNT (2,4,6-trinitrotoluene) and CL-20(2,4,6,8,10,12-hexanitrohexaazaisowurtzitane) [116]. Three kinds of mixing models were created as follows: 1) An amorphous cell containing eight TNT molecules and eight CL-20 molecules was created by Amorphous cell module. The density of the cell was set as 1.91g/cm^3, the same with of TNT/Cl-20 cocrystal. 2) A periodic box of 200Å×200Å×200Å was created, a supper cell of TNT(2×3×1) and CL-20(3×2×2) were put into the box. Then, the MD simulation was carried out in normal volume and temperature (NVT) conditions for 20ps with COMPASS force field to reach the equilibrium state. After that, they reduced the volume of the box gradually and performed the calculation repeatedly until the density reached to 1.91g/cm^3. 3) The main planes of TNT and CL-20 were predicted by Morphology module and the crystals were cleaved by the most important face, respectively. A layer combining a supper cell of TNT(2×3) and CL-20(3×2) was made. After the equilibrium of the system, the average bond length of trigger bond (L_{ave}) is almost unchanged after mixing or cocrystallization. However, the largest bond length of trigger bond (L_{max}) of CL-20 in cocrystal is shorter than that of it in pure CL-20, which indicates that the cocrystal is more difficult to be detonated than CL-20. The L_{max} of TNT shows the same result. The cocrystal shows a larger cohesive energy density than composite ones, suggesting the cocrystal is more insensitive. Besides, trigger bond energy of cocrystal is larger than physical mixture of TNT and CL-20, suggesting the cocrystal is more insensitive. The results show that the mechanical properties of the cocrystal are more harder than pure TNT or CL-20, but has a weaker ductibility and tenacity.

Formation of cocrystals having high-energy low-sensitivity explosives are research objectives in the field of energetic materials, and the cocrystals of that sort is an important method to improve the safety of explosives. However, the sensitivity reduction mechanism of cocrystal explosives is still unclear. In the work Wang *et al.*, CL-20/TNT, CL-20 and TNT crystals were taken as the research objects. They used the data excerpted from the literature results of X-ray single-crystal diffraction experiments, and the unit-cell structures of CL-20/TNT, CL-20 and TNT crystals were established. Then, by simulating with ReaxFF-lg reactive force field they investigated the propagation process of the wave front in the crystals at different impact velocities [117]. The molecular dynamics data were used to analyze the molecular structure changes and initial chemical reactions, and to explore the sensitivity reduction mechanism of the CL-20/TNT cocrystal. The results have revealed that the chemical reaction of the CL-20/TNT cocrystal, compared with the CL-20 single crystal, is different under different impact velocities. When the CL-20/TNT cocrystal was impacted at low velocity (e.g, 2 km/s), polymerization and separation of the component molecules easily occurred, which weakened the decomposition of the CL-20 molecules. At a medium impact velocity (3 km/s), the decay rates of CL-20 and TNT in the cocrystal decreased, prolonging the primary reaction process and promoting formation of the intermediate products (such as nitrogen oxides). At a high impact velocity (4 km/s), the cocrystal had little effect on the decay rates of the molecules and formation of CO_2, but it enhanced the formation of N_2 and H_2O. This may explain the reason for the impact-sensitivity reduction of the CL-20/TNT cocrystal. At an impact velocity of 2 km/s, polymerization and separation of the component molecules weakened the decomposition of CL-20. At an impact velocity of 3 km/s, the decay rates of CL-20 and TNT in the cocrystal decreased, and the formation of intermediate products were enhanced, such as nitrogen oxides. Whereas at an impact velocity of 4 km/s, the cocrystal exhibited little effect on the decay rates of the molecules and formation of CO_2, but it enhanced formation of N_2 and H_2O. This may explain why the impact-sensitivity of the CL-20/TNT cocrystal reduces [117].

Cocrystals of CL-20 with 1,4-DNI

The emerging of an energetic cocrystal technique provides a potential opportunity to synthesize and construct new energetic compounds. Of the dinitroimidazole isomers, 1,4-dinitroimidazole ((1,4-DNI) has been considered for cocrystalization with CL-20.

1,4-DNI

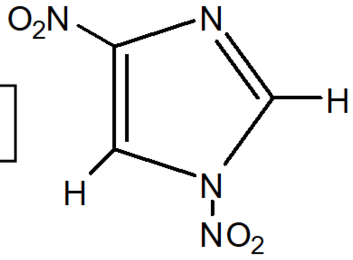

In the work of Tan *et al.,* a new 1:1 cocrystal explosive composed of 2,4,6,8,10,12-hexanitrohexaazaiso-wurtzitane (CL-20) and 1,4-dinitroimidazole (1,4-DNI) was synthesized through cocrystallization by slow solvent evaporation (ethyl acetate at room temperature) [118]. Single crystal X-ray diffraction (SXRD) and powder X-ray diffraction (PXRD) analyses were done. The data revealed that the cocrystal has a crystal density of 1.922 g/cm^3 at 296 °K and belongs to the orthorhombic system with P212121 space group. The properties of the cocrystal including thermal stability, impact sensitivity, and detonation performances were studied. The DSC test shows that the cocrystal has a melting point of 115 °C with a decomposition temperature of 253 °C, which suggests an excellent thermal stability. The detonation velocity and pressure of the cocrystal were calculated according to the calculation method of the empirical nitrogen equivalent equations [119]. For comparisons, ε-CL-20, 1,4-DNI, HMX, CL-20/TNT cocrystal, and CL-20/DNB cocrystal were also calculated by the same method. The results show that the cocrystal exhibits an impact energy with 50% ignition probability of 10 J, showing a substantial reduction in impact sensitivity compared to pure CL-20 and HMX. The predicted detonation velocity and detonation pressure of the cocrystal are 9242 m/s and 39.01 GPa, respectively, which are similar to those of HMX. Therefore, the authors contemplate that the CL-20/1,4-DNI cocrystal may be an attractive high energy explosive with low sensitivity thus, may act as a promising explosive candidate instead of HMX for low vulnerability formulations in the future.

In the work of Li *et al.*, the CL-20/1,4-DNI unit cell structure was geometrically optimized by the COMPASS force field [120]. The AE model was used to predict the morphology of CL-20/1,4-DNI under vacuum, resulting in the most morphologically important growth planes. Ethyl acetate was selected as the solvent. The interaction energy between the solvent and the crystal plane, and the attachment energies in solvent at 298°K, 320°K, 340°K, 360°K, and 380°K were predicted. The morphologies of hexanitrohexaazaisowurtzitane (CL-20) and 1,4-dinitroimidazole (1,4-DNI) co-crystal under vacuum or solvent at different temperatures were predicted. The NVT ensemble is used in the molecular dynamics calculation process. The simulation step is 1 fs and the total simulation time is 500 ps. The Andersen thermostat is selected as the temperature control method. In the potential energy calculation, the atom-based and Ewald methods were selected to calculate the van der Waals force and the electrostatic interaction force, respectively.

The CL-20/1,4-DNI co-crystal has six important growth crystal planes, namely (002), (011), (101), (11–1), (110), (111). The areas of (002), (101), and (011) planes account for a relatively large proportion, which are important crystal planes that affect the crystal morphology. Also the crystal habits at different temperatures were simulated. The simulation results revealed that the crystal plane attachment energy of CL-20 and 1,4-DNI co-crystal increases with the increase of temperature, indicating that the increase of temperature is conducive to the growth of crystal planes. On the other hand, the aspect ratio decreases with the increase of temperature and the morphology of co-crystal becomes more spherical at a higher temperature. The results showed that the theoretical predictions are in good agreement with the experiment. The simulation results can provide guidance for the crystallization of CL-20/1,4-DNI to obtain a nearly spherical crystal morphology [120].

In the study of Dong *et al.*, the thermodynamic criterion for the cocrystal formation has been investigated considering the thermodynamic of hexanitrohexaazaisowurtzitane (CL-20)/1,4-dinitroimidazole (1,4-DNI) cocrystal formation to provide the theoretical basis for the screening and optimization of crystallization solvents and parameters [121]. As solvents; acetone, ethyl acetate and methanol were used. The solubility data of CL-20, 1,4-DNI in pure solvents and CL-20 in 1,4-DNI solutions with different concentrations (0.04, 0.06, 0.08, 0.10, 0.12, 0.16, 0.20, 0.24 $g \cdot mL^{-1}$) were achieved with the help of high performance liquid chromatography. The ternary phase diagrams of CL-20/1,4-DNI solvents were built. The thermodynamic parameters of the solubility product K_{sp}, the complexation constant K_{11}, and the reaction free energy ΔG^0 were obtained through fitting the solubility data based on the mathematical models of solution chemistry theory [121]. The results have shown that if the solubilities of CL-20 and 1,4-DNI are larger and their discrepancy is less in a solvent, the cocrystal region is larger and its shape is more symmetrical. The order of the cocrystal regions in the three solvents (ranging from large to small) is acetone > ethyl acetate > methanol. The shape of the cocrystal region in the acetone and ethyl acetate is more symmetrical. Among the three solvents employed, the calculated thermodynamic parameters indicate that the acetone is the most beneficial to the formation of CL-20/1,4-DNI cocrystal, followed by ethyl acetate. The ternary phase diagram and thermodynamic parameters in acetone solvent at different temperatures reveal that lowering the crystallization temperature is beneficial to the precipitation of the CL-20/1,4-DNI cocrystal [121].

In the work, by Xu, *et al.*, all cocrystals have been synthesized and downloaded from the Cambridge Crystallographic Data Centre (CCDC) and all the calculations were performed with the Gaussian 16 software package [122]. The B3LYP-D3/6–311 + G(d,p) method was used to fully optimize the molecular structures of the three cocrystals under the EEF and no EEF. The cocrystals considered are (CL-20/1,4-DNI), HNIW/1-methyl-2,4-dinitro-1H-imidazole (CL-20/2,4-MDNI) and HNIW/1-methyl-4,5-dinitro-1H-imidazole (CL-20/4,5-MDNI). It has been found that the external electric field (EEF) has a significant influence on the sensitivity of the energetic cocrystal materials. In this work, density functional theory (DFT) at B3LYP-D3/6–311 + G(d,p) and M062X-D3/ma-def2 TZVPP levels were employed to calculate the bond dissociation energies (EBDE) of selected N-NO_2 trigger bonds, frontier molecular orbitals, electrostatic potentials (ESPs) and nitro group charges (QNO_2) under different EEF. The results show that as the positive electric field increases, the highest occupied molecular orbital (HOMO) and the lowest unoccupied molecular orbital (LUMO) energy gap and EBDE become smaller, and the local positive ESPs becomes larger so that the energetic cocrystals tends to have higher sensitivity. In addition, the linear fitting results show that the trigger bond length and nitro group charge changes are closely related to the EEF [122].

Cocrystals of CL-20 with NQ

Nitroguanidine (NQ) is one of the insensitive energetic compounds which is investigated for the cocrystalization purposes. Earlier, Gao *et al.,* in one of their work considered nano-sized CL-20/NQ co-crystal [33].

NQ

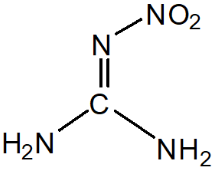

Nano-sized energetic materials with spherical shape were proved to have lower initiation sensitivity and reduced critical diameter in recent publications [123-126]. Besides, nano-sized energetic materials have been used in some kinds of polymer bonded explosive (PBX) [127] and composite modified double-base propellant (CMDB) [128] to bring high energy and low sensitivity together. Therefore, if co-crystallization and nano technology can be combined, it will be more promising for energetic co-crystals used in military and civilian applications. NQ, an important industrial raw material which has two different structures, is usually used as a component of rockets, missiles and bullets [129-131]. Nano-sized energetic co-crystal consisting of CL-20 (the most powerful used military explosive 2,4,6,8,10,12-hexanitro-2,4,6,8,10,12-hexaazaisowurtzitane) and a typical insensitive explosive used in propellants nitroguanidine (NQ) was prepared by the vacuum freeze drying method. Note that the vacuum freeze drying, (which also called sublimation drying), has been widely used in the food industry and raw material production [132-133]. Its principle is to freeze the solvent in the material to solid state (like water into ice) and then make the solvent sublimate directly under vacuum condition to achieve the purpose of drying. The fine particles of material cannot grow and reunite in solid state solvent so that vacuum freeze drying is an effective way to prepare nano-sized material. Material studio 6.1 was used to simulate the hydrogen bonds between CL-20 and NQ molecules. Scanning electron microscopy (SEM) was used to reveal the morphology and size of the product. Fourier Transform infrared spectroscopy (FT-IR) and X-ray diffraction spectrum (XRD) proved the formation of the co-crystal at the molecular level. Differential scanning calorimetry (DSC) was employed to characterize the thermal behavior of the co-crystal obtained. The result of mechanical sensitivity test indicated that the sensitivity was effectively reduced compared to neat CL-20 [33].

Cocrystals of CL-20 with BTF

Yin *et al.,* considered CL-20/BTF (HNIW/benzotrifuroxan) cocrystal as a typical cocrystal explosive to investigate its thermal kinetics and decomposition mechanism. The thermal behavior of CL-20/BTF shows no phase transition or solid–liquid melting process before decomposition, which is distinct from those of pure CL-20 and BTF crystals. Further, they identified the thermal decomposition of CL-20/BTF as a particular reaction kinetics consisting of two parallel autocatalytic paths. The contribution of these two paths to the overall reaction varies with the change of heating rate. Based on the established kinetic model, important thermal safety indicators including TMRad and SADT are simulated. Finally, in situ infrared spectroscopy was performed to detect the molecular evolution of CL-20/BTF cocrystal during thermal decomposition, which is helpful to understand the origin of its thermal kinetics. It is found that the unique decomposition mechanism of strong intermolecular coupling between CL-20 and BTF molecules is responsible for the parallel reaction paths of the thermal kinetics of the CL-20/BTF cocrystal [134].

BTF

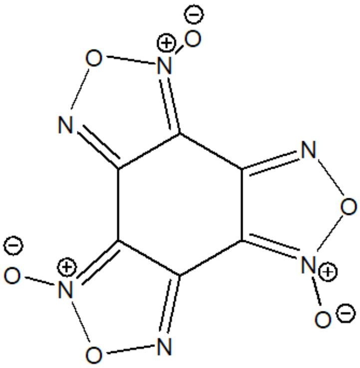

In order to find out the relationship between the external electric field and sensitivity of cocrystals 2,4,6,8,10,12-hexanitro-2,4,6,8,10,12-hexaazaiso wurtzitane /benzotrifuroxan (CL-20/BTF), Hao *et al.*, in their work considered the density functional theory at B3LYP-D3/6-311+G(d,p) and M062X-D3/ma-def2 TZVPP levels to calculate the frontier molecular orbitals, atoms in molecules (AIM), electron density values, bond dissociation energies (BDEs) of the N–NO2 bond, impact sensitivity (H_{50}), electrostatic potentials (ESPs), and nitro group charges (Q_{NO2}) [135]. The results show that a smaller highest occupied molecular orbital–lowest unoccupied molecular orbital gap and the BDEs, as well as H_{50}, tend to have a larger sensitivity along with the positive directions in the external electric field. Moreover, a smaller local positive ESP ($V_{\mathrm{s\ max}}$) leads to better stability in the negative electric field. The sensitivity of cocrystal molecules decreases gradually in the negative external electric field with the increase of negative nitro group charges. Finally, it has been found that the change in the bond lengths, AIM electron density values, and nitro group charges correlate well with the external electric field strengths [135].

Li *et al.*, performed some density functional theory (DFT) simulations to investigate how the structure, interaction and mechanical properties of 2,4,6,8,10,12-hexanitro-2,4,6,8,10,12-hexaazaisowurtzitane/benzotrifuroxan (CL-20/BTF) behave under a hydrostatic pressure in the range of 0–100 GPa. The calculated structure agrees well with the experimental data at ambient pressure and 293 °K. Whereas, the CL-20/BTF cocrystal exhibits an anisotropic compression behavior (as shown by the change in lattice constants with pressure) because it is more difficult to compress along the *b*-axis. Moreover, the band gap values decrease rapidly in the range of 0 GPa to 40 Gpa and then decrease slowly with increasing pressure from 50 GPa to 100 GPa. Furthermore, the analysis of the active bond reveals that two types of O–N bonds in the furoxan group and four types of N–N bonds in CL-20 have significant response to the applied pressure. The results have revealed that the Hirshfeld surface can give an insight into intermolecular interaction. By combining the analysis of the Hirshfeld surface with two-dimensional fingerprint plots shows that intermolecular interaction mainly comes from hydrogen bonding interactions and NO_2–π interaction in CL-20/BTF cocrystal. According to the stronger intermolecular interaction (sum of O···H/H···O, N···H/H···N, O···N/N···O and O···O) decreasing with increasing pressure, one can speculate that the impact sensitivity of CL-20/BTF increases as the pressure increases. Investigation of the mechanical properties reveals that this cocrystal shows an increase in ductility, deformation resistance and stiffness with increasing pressure. On the other hand, the elastic anisotropy indicates that the CL-20/BTF cocrystal varies anisotropically under pressure in the range of 0–100 GPa but is near isotropy level under 20 GPa [136].

Cocrystals of CL-20 with LLM-105

LLM-105 is the abbreviation for 2,6-Diamino-3,5-Dinitropyrazine-1-Oxide (LLM-105). It is a relatively new and promising insensitive high-explosive (IHE) material. Hamilton *et al.*, adopted a multitheory approach based on reactive molecular dynamic simulations performed with density functional theory, density functional tight-binding, and reactive force fields to characterize the reaction pathways, product speciation, reaction kinetics, and detonation performance of LLM-105 [137]. They have found that the early reaction pathways of LLM-105 decomposition are extremely similar to TATB; both of which involve intra- and intermolecular hydrogen transfer. Additionally, the detonation performance of LLM-105 falls between that of TATB and HMX. The authors have found an agreement between the predictive models for first step reaction pathways but significant differences in final product formations [137].

LLM-105

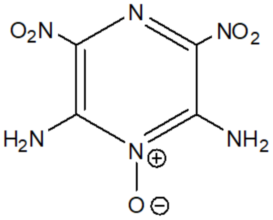

Cocrystal explosive can effectively improve the physical and chemical properties of explosive and contributed to new unique properties of cocrystal explosive. In the work by Zhang *et al.*, (based on cocrystal principle) a few recrystallization explosives of LLM-105 were prepared by using the special solvent/non-solvent technique [138]. Since, the solubility difference was large among the explosive components in different solvents, especially in the case of LLM-105, it was very important to choice the proper crystallization solvent system and the control of the crystallization conditions.

The experimental results showed that the system of LLM-105 and HNIW failed to form cocrystal with a single pure DMSO as solvent system. However, when they were joined with trifluoroacetic acid, the system of LLM-105 and HNIW formed cocrystal. It is true that trifluoroacetic acid damages the hydrogen bonds of LLM-105, resulting in the LLM-105 and HNIW forming new hydrogen bonding force between the two components [138]. Therefore, the mixed solvent, as solvent of cocrystal explosive system has significant effect on cocrystal explosive system, which can greatly broaden the cocrystal explosive composition and scope of the choice of solvent system.

The prepared samples in the work were analyzed by IR spectroscopy. The results revealed that cocrystals such as LLM-105/HNIW (LLM-105/CL-20), LLM-105/HMX and LLM-105/RDX can be prepared. Melting point and density of the abovementioned cocrystals changed little. It can be inferred the cocrystal explosive will have better energy and their application performances will not reduce obviously [138].

In one of articles by Hang *et al.*, the hexanitrohexaazaisowurtzitane/2,6-diamino-3,5-dinitropyrazine-1-oxide (CL-20/LLM-105) cocrystal models with different component ratios were reported [139]. The cocrystals were obtained by the substitution method. The stability, sensitivity, energetic performance, and mechanical properties of CL-20, LLM-105, and CL-20/LLM-105 cocrystal models were predicted by the molecular dynamics method [139]. The results revealed that the CL-20/LLM-105 cocrystal model with component ratio of 2:1 has the highest value of binding energy and is the most stable model. The authors obtained that the cocrystal model had shorter trigger bond length than pure CL-20, but higher value of trigger bond energy and cohesive energy density. These results imply that the sensitivity of cocrystal explosive should have decreased. The cocrystal explosive has lower energy density than CL-20, but the cocrystal explosive with molar ratio of 10:1~2:1 still has high energy density and can be regarded as novel high energy density compound (HEDC). Also the tensile modulus, shear modulus, and bulk modulus of the cocrystal models are decreased. However, Cauchy pressure is increased, that means the mechanical properties are improved. In the light of all these, the authors have reached a conclusion that CL-20/LLM-105 cocrystal explosive with component ratio of 2:1 has the best stability, lowest mechanical sensitivity, most desirable mechanical properties, and high energy density [139]. Thus, it is very promising to become a novel HEDC.

Conclusion

In the energetic material community, energetic cocrystals represent one of the most important research interests. The preparation and characterization procedures for some energetic cocrystals have been established and still slowly being developed, however, there are still some fundamental problems associated with structure‑property relationships of energetic cocrystals that needed to be explored. Densities of energetic cocrystals usually tend to fall between those of the precursors. In some rare examples of CHNO energetic cocrystals there are some reports that cocrystals having higher density than all coformers. Hence, further studies are expected to increase packing coefficient and enhance the density to a higher level for energetic cocrystals. In addition, the heats of formation of most reported energetic cocrystals are theoretically determined. Since those are important parameters for accurate evaluation of detonation performances, the use of high precision calculation methods as well as experimental measurements are needed.

In summary, cocrystal technology can effectively improve the properties of explosives. Researchers actively apply supramolecular cocrystallization to the field of energetic materials, and explore the designing, characterization, prediction and synthesis of new high-energy insensitive explosives in the light of theoretical calculations and experiments.

References

[1] Dong, H., & Zhou, F. (1994). *Properties of high energetic explosives and relatives*, Beijing: Science Press.

[2] Türker, L. (2019). Nitramine derivatives of NTO – A DFT study. *Earthline Journal of Chemical Sciences, 1*(1), 45-63. https://doi.org/10.34198/ejcs.1119.4563

[3] Türker, L. (2011). Recent developments in the theory of explosive materials, (In T.J. Jansen (Ed.)), *Explosive materials, materials science and technologies*). New York: Nova Science Pub.

[4] Türker, L., & Variş, S. (2009). A review of polycyclic aromatic energetic materials. *Polycyclic Aromatic Compounds*, *29*(4), 228-266. https://doi.org/10.1080/10406630903135971

[5] Türker, L. (2019). Interaction of CL-20 and zinc - A DFT treatment. *Earthline Journal of Chemical Sciences*, *2*(2), 205-215. https://doi.org/10.34198/ejcs.2219.205215

[6] Türker, L. (2021). Some novel tricyclic caged-nitramines - A DFT study. *Earthline Journal of Chemical Sciences*, *5*(1), 35-48. https://doi.org/10.34198/ejcs.5121.3548

[7] Teipel, U. (2005). *Energetic materials. Particle processing and characterization.* WILEY-VCH Verlag GmbH & Co. KGaA.

[8] Fried, L.E., Manaa, M.R., Pagoria, P.F., & Simpson, R.L. (2001). Design and synthesis of energetic materials. *Annu. Rev. Mater. Res.*, *31*, 291-321. https://doi.org/10.1146/annurev.matsci.31.1.291

[9] Gao, H.X., & Shreeve, J.M. (2011). Azole-based energetic salts. *Chem. Rev.*, *111*, 7377-7436. https://doi.org/10.1021/cr200039c

[10] Wang, X., Xu, K., Sun, Q., Wang, B., Zhou, C., & Zhao, F. (2015). The insensitive energetic material trifurazano-oxacycloheptatriene (TFO): Synthesis and detonation properties. *Propellants, Explos., Pyrotech*., *40*, 9-12. https://doi.org/10.1002/prep.201400148

[11] Talawar, M.B., Sivabalan, R., Senthilkumar, N., Prabhu, G., & Asthana, S.N. (2004). Synthesis, characterization and thermal studies on furazan- and tetrazine-based high energy materials. *J. Hazard. Mater*., *113*, 11-25. https://doi.org/10.1016/j.jhazmat.2004.05.016

[12] Chen, H., Li, L., Jin, S., Chen, S., & Jiao, Q. (2012). Effects of additives on ε-HNIW crystal morphology and impact sensitivity. *Propellants, Explos., Pyrotech*., *37*, 77-82. https://doi.org/10.1002/prep.201000014

[13] Wang, Q.Y., Feng, X., Wang, S., Song, N., Chen, Y., Tong, W., Han, Y., Yang, L., & Wang, B. (2016). Metal-organic framework templated synthesis of copper azide as the primary explosive with low electrostatic sensitivity and excellent initiation ability. *Adv. Mater*., *28*, 5837-5843. https://doi.org/10.1002/adma.201670192

[14] Xue, Z-H., Zhang, X-X., Huang, B. B., & Xin B. (2020). The structural diversity of hybrid qy-HMX crystals with constraint of 2D dopants and the resulted changes in thermal reactivity. *Chem. Eng. J*., *390*, 124565. https://doi.org/10.1016/j.cej.2020.124565

[15] Nangia, A. (2004). Nomenclature in crystal engineering. In J. L. Atwood & J. W. Steed (Eds.), *Encyclopedia of supramolecular chemistry* (Vol. 2). New York: Marcel Dekker.

[16] Dunitz, J.D. (2003). Crystal and co-crystal: a second opinion. *Cryst. Eng. Comm., 5*, 506-506. https://doi.org/10.1039/B315687G

[17] Vishweshwar, P., Mcmahon, J.A., Bis, J.A., & Zaworotko, M.J. (2006). Pharmaceutical co-crystals. *J. Pharma. Sci.*, *95*, 499-516. https://doi.org/10.1002/jps.20578

[18] Desiraju, G.R. (2003). Crystal and co-crystal. *Cryst. Eng. Comm., 5*, 466-467. https://doi.org/10.1039/b313552g

[19] Aakeröy, C.B., & Salmon, D.J. (2005). Building co-crystals with molecular sense and supramolecular sensibility. *Cryst. Eng. Comm., 7* (72), 439-448.

[20] Liu, G.R., Li, H.Z., Gou, R.J., & Zhang, C. (2018). Packing structures of CL-20-based cocrystals. *Cryst. Growth Des.*, *18*, 7065-7078. https://doi.org/10.1021/acs.cgd.8b01228

[21] Liu, G., Wei, S-H., & Zhang, C. (2020). Review of the intermolecular interactions in energetic molecular cocrystals. *Cryst. Growth Des.*, *20*(10), 7065-7079. https://doi.org/10.1021/acs.cgd.0c01097

[22] Zhang, C., Xiong, Y., Jiao, F., Wang, M., & Li, H. (2019). Redefining the term of cocrystal and broadening its intension. *Cryst. Growth Des.*, *19*, 1471-1478. https://doi.org/10.1021/acs.cgd.8b01537

[23] Liu, K., Zhang, G., Chen, Z.Q., Luan, J., & Xu, M. (2014). Research progress of cocrystal energetic materials. *Chemical Analysis and Meterage.*, *5*, 139-142.

[24] Fleischman, S.G., Kuduva, S.S., McMahon, J.A., Moulton, B., Bailey W., Rosa, D., Naír, R-H., & Zaworotko, M.J. (2003). Crystal engineering of the composition of pharmaceutical phases: Multiple-component crystalline solids involving carbamazepine. *Cryst. Growth Des.*, *3*, 909-919. https://doi.org/10.1021/cg034035x

[25] Lara-Ochoa, F., & Espinosa-Perez, G. (2007). Cocrystals definitions. *Supramol. Chem.*, *19*, 553-557. https://doi.org/10.1080/10610270701501652

[26] Aitipamula, S., Banerjee, R., Bansal, A.K., Biradha, K., Cheney, M. L., Choudhury, A.R., Desiraju, G.R., Dikundwar, A.G., Dubey, R., Duggirala, N., Ghogale, P.P., Ghosh, S., Goswami, P.K., Goud, N.R., Jetti, R.R.K.R., Karpinski, P., Kaushik, P., Kumar, D., Kumar, V., Moulton, B., Mukherjee, A., Mukherjee, G., Myerson, A.S., Puri, V., Ramanan, A., Rajamannar, T., Reddy, C.M., Rodriguez-Hornedo, Nair., Rogers, R.D., Row, T.N.G., Sanphui, P., Shan, N., Shete, G., Singh, A., Sun, C.C., Swift, J.A., Thaimattam, R., Thakur, T.S., Thaper, R.K., Thomas, S.P., Tothadi, S., Vangala, V.R., Variankaval, N., Vishweshwar, P., Weyna, D.R., & Zaworotko, M.J. (2012). Polymorphs, salts, and cocrystals: What's in a name. *Cryst. Growth Des.*, *12*, 2147-2152. https://doi.org/10.1021/cg3002948

[27] Ma, Q., Huang, S., Lu, H., Nie, F., Liao, L., Fan, G., & Huang, J. (2019). Energetic cocrystal, ionic salt, and coordination polymer of a perchlorate free high energy density oxidizer: Influence of pKa modulation on their formation. *Crystal Growth & Design, 19*, 714-723. https://doi.org/10.1021/acs.cgd.8b01293

[28] Xue, Z-H., Huang, B., Li, H., & Yan, Q-L. (2020). Nitramine-based energetic cocrystals with improved stability and controlled reactivity. *Crystal Growth & Design*, *20* (12), 8124-8147. https://doi.org/10.1021/acs.cgd.0c01122

[29] Shan, N., & Zaworotko, M.J. (2008). The role of cocrystals in pharmaceutical science. *Drug Discovery Today*, *13*, 440-446. https://doi.org/10.1016/j.drudis.2008.03.004

[30] Bu, R.P., Xiong,Y.,Wei, X.F., Li, H., & Zhang, C. (2019). Hydrogen bonding in CHON-

contained energetic crystals: A review. *Cryst. Growth Des.*, *19*, 5981-5997. https://doi.org/10.1021/acs.cgd.9b00853

[31] Ghosh, M., Sikder, A.K., Banerjee, S., & Gonnade, R.G. (2018). Studies on CL-20/HMX (2:1) Cocrystal: A new preparation method and structural and thermokinetic analysis. *Cryst. Growth Des.*, *18*, 3781-3793. https://doi.org/10.1021/acs.cgd.8b00015

[32] Parakhin, V.V., & Smirnov, G.A. (2024). Research progress on design, synthesis and performance of energetic polynitro hexaazaisowurtzitane derivatives: Towards improved CL-20 analogues. *FirePhysChem., 4*(1), 21-33. https://doi.org/10.1016/j.fpc.2023.05.006 .

[33] Gao, H., Du, P., Ke, X., Liu, J., Hao, G., Chen, T., & Jiang, W. (2017). A novel method to prepare nanosized CL-20/NQ co-crystal: vacuum freeze drying. *Propellants, Explos., Pyrotech., 42,* 889-895. https://doi.org/10.1002/prep.201700006

[34] Landenberger, K.B., & Matzger, A.J. (2010). Cocrystal engineering of a prototype energetic material: Supramolecular chemistry of 2,4,6-trinitrotoluene. *Cryst. Growth Des.*, *10*, 5341-5347. https://doi.org/10.1021/cg101300n

[35] Liu, N., Duan, B., Lu, X., Mo, H., Xu, M., Zhang, Q., & Wang, B. (2018). Preparation of CL-20/DNDAP cocrystals by a rapid and continuous spray drying method: an alternative to cocrystal formation. *Cryst. Eng. Comm.*, *20*, 2060-7. https://doi.org/10.1039/C8CE00006A

[36] An, C., Li, H., Ye, B., & Wang, J. (2017). Nano-CL-20/HMX cocrystal explosive for significantly reduced mechanical sensitivity. *J. Nanomater.*, 3791320-7. https://doi.org/10.1155/2017/3791320

[37] Liu J., Yan, Z., Chi, D., & Yang, L. (2019). Synthesis of the microspheric cocrystal CL-20/2,4-DNI with high energy and low sensitivity by a spray-drying process. *N.J. Chem.*, *43*(44), 17390-4. https://doi.org/10.1039/C9NJ04731J

[38] Qiu, H., Patel, R.B., Damavarapu, R.S., & Stepanov, V. (2015). Nanoscale 2CL-20.HMX high explosive cocrystal synthesized by bead milling. *Cryst. Eng. Comm.*, *17*(22), 4080-3. https://doi.org/10.1039/C5CE00489F

[39] Hu,Y., Yuan, S., Li, X., Liu, M., Sun, F., Yang, Y., Hao,G., & Jiang,W. (2020). Preparation and characterization of nano-CL-20/TNT cocrystal explosives by mechanical ball-milling method. *ACS Omega., 5*, 17761-6. https://doi.org/10.1021/acsomega.0c02426

[40] Huang, C., Xu, J., Tian, X., Liu, J., Pan, L., Yang, Z., & Nie, F. (2018). High-yielding and continuous fabrication of nanosized CL-20-based energetic cocrystals via electro spraying deposition. *Cryst. Growth. Des., 18*, 2121-8.

https://doi.org/10.1021/acs.cgd.7b01568

[41] Liu, N., Duan, B., Lu, X., Mo, H., Bi, F., Wang B., Zhang, J., & Yan, Q-L. (2019). Rapid and high-yielding formation of CL-20/DNDAP cocrystals via self-assembly in slightly soluble-medium with improved sensitivity and thermal stability. *Propell., Explos., Pyrot.*, *44*, 1242-53. https://doi.org/10.1002/prep.201900053

[42] Zhang, M., Tan, Y., Zhao, X., Zhang, J., Huang, S., Zhai, Z., Liu, Y., & Yang, Z. (2020). Seeking a novel energetic cocrystal strategy through the interfacial self-assembly of CL-20 and HMX nanocrystals. *Cryst. Eng. Comm.*, *22*, 61-7. https://doi.org/10.1039/C9CE01447K

[43] Li, L., Ling, H., Tao, J., Pei, C., & Duan, X. (2022). Microchannel-confined crystallization: shape-controlled continuous preparation of a high-quality CL-20/HMX cocrystal. *Cryst. Eng. Comm.*, *24*(8), 1523-8. https://doi.org/10.1039/D1CE01524A

[44] Viswanath, J.V., Shanigaram, B., Vijayadarshan, P., Chowadary, T.V., Gupta, A., Bhanuprakash, K., Niranjana, S.R., & Venkataraman, A. (2019). Studies and theoretical optimization of CL-20: RDX cocrystal. *Propellants, Explos., Pyrotech.*, *44*, 1570-1582. https://doi.org/10.1002/prep.201900126

[45] Trache, D., Klapotke, T.M., Maiz, L., And-Elghany, M., & DeLuca, L.T. (2017). Recent advances in new oxidizers for solid rocket propulsion. *Green Chem.*, *19*, 4711-4736. https://doi.org/10.1039/C7GC01928A

[46] Viswanath, J.V., Venugopal, K.J., Srinivasa R.N.V., & Venkataraman, A. (2016). An overview on importance, synthetic strategies and studies of 2,4,6,8,10,12-hexanitro-2,4,6,8,10,12-hexaazaisowurtzitane (HNIW). *Defence Technology.*, *12*, 401-418. https://doi.org/10.1016/j.dt.2016.05.002

[47] Viswanath, J.V., Vijayadarshan, P., Mohan, T., Srinivasa, R.N.V., Gupta, A., & Venkataraman, A. (2017). Copper chromite as ballistic modifier in a typical solid rocket propellant composition: A novel synthetic route involved. *J. Energ. Mater.*, *36*, 69-81. https://doi.org/10.1080/07370652.2017.1313911

[48] Gao, H., Jiang, W., Liu, J., Hao, G., Xiao, L., Ke, X., & Chen, T. (2017). Synthesis and characterization of new co-crystal explosive with high energy and good sensitivity. *J. Energ. Mater.*, *35*, 490-498. https://doi.org/10.1080/07370652.2017.1290712

[49] Wei, X., Zhang, A., Ma, Y., Xue, X., Zhou, J., Zhu, Y., & Zhang, C. (2015). Towards low-sensitive and high-energetic cocrystal III: thermodynamics of energetic-energetic cocrystal formation. *Cryst. Eng. Comm.*, *17*, 9037-9047. https://doi.org/10.1039/C5CE02009C

[50] Yang, Z., Li, H., Zhou, X., Zhang, C., Huang, H., Li, J., & Nie, F. (2012). Characterization and properties of a novel energetic-energetic cocrystal explosive exposed of HNIW and BTF. *Cryst. Growth Des.*, *12*, 5155-5158. https://doi.org/10.1021/cg300955q

[51] Song, X.L., Wang, Y., Zhao, S., & Li, F. (2018). Mechanochemical fabrication and properties of CL-20/RDX nano co/mixed crystals. *RSC Adv.*, *8*, 34126-34135. https://doi.org/10.1039/C8RA04122A

[52] Hang, G-Y., Yu, W-l., Wang, T., Wang, J-T., & Li, Z. (2017). Theoretical insights into effects of molar ratios on stabilities, mechanical properties and detonation performance of CL-20/RDX cocrystal explosives by molecular dynamics simulation. *Journal of Molecular Structure*. *1141*, 577-583.

[53] Wang, F., Du, G., Liu, X., Shao, M., Zhang, C., & Chen, L. (2022). Molecular dynamics application of cocrystal energetic materials: A review. *Nanotechnology Reviews*, *11*, 2141-2153. https://doi.org/10.1515/ntrev-2022-0124

[54] Shutao, W., Shifa, C., Siqi, L., Di, W., & Xiaohan, S. (2023). The MD calculation of the cocrystal of CL-20/RDX. *Proceedings of the SPIE*, 12636, id. 1263632 -7. https://doi.org/10.1117/12.2675198

[55] Bolton, O., Simke, L.R., Pagoria, P.F., & Matzger, A.J. (2012). High power explosive with good sensitivity: a 2:1 cocrystal of CL-20: HMX. *Cryst. Growth Des.*, *12*, 4311-4314. https://doi.org/10.1021/cg3010882

[56] Liu, Z-C., Wu, Q., Zhu, W-H., & Xiao, H. (2015). Insights into the roles of two constituents CL-20 and HMX in the CL-20:HMX cocrystal at high pressure: a DFT-D study. *RSC Adv.*, *5*, 34216-34225. https://doi.org/10.1039/C5RA01829C

[57] Sun, S.H., Zhang, H.B., Liu, Y., Xu, J., Huang, S., Wang, S., & Sun, J. (2018). Transitions from separately crystallized CL-20 and HMX to CL-20/HMX cocrystal based on solvent media. *Cryst. Growth Des.*, *18*, 77-84. https://doi.org/10.1021/acs.cgd.7b00775

[58] Zhao, L., Yin, Y., Sui, H., Yu, Q., Sun, S., Zhang, H., Wang, S., Chen, L., & Sun, J. (2019). Kinetic model of thermal decomposition of CL-20/HMX co-crystal for thermal safety prediction. *Thermochimica Acta*, *674*, 44-51. https://doi.org/10.1016/j.tca.2019.02.001

[59] Sun, T., Xiao, J.J., Liu, Q., Zhao, F., & Xiao, H.M. (2014). Comparative study on structure, energetic and mechanical properties of a ε-CL-20/HMX cocrystal and its composite with molecular dynamics simulation. *J. Mater. Chem.* A, *2*, 13898-13904. https://doi.org/10.1039/C4TA01150C

[60] Ding, L., Zhao, F.Q., & Liu, Z.R. (2008). Thermal decomposition of CL- 20/HMX mixed system. *J. Solid Rocket Technol*., *31*(2), 164-167.

[61] Kim, S.B., Kim, K.J., Cho, M.H., Kim, J.H., Kim, K.T., & Kim, S.H. (2016). Micro- and nanoscale energetic materials as effective heat energy sources for enhanced gas generators. *ACS Appl. Mater. Interfaces*, *8*, 9405-9412. https://doi.org/10.1021/acsami.6b00070

[62] Myers, T.W., Bjorgaard, J.A., Brown, K.E., Chavez, D.E., Hanson, S.K., Scharff, R.J., Tretiak, S., & Veauthier, J.M. (2016). Energetic chromophores: low-energy laser initiation in explosive Fe(II) tetrazine complexes. *J. Am. Chem. Soc*., *138*, 4685-4692. https://doi.org/10.1021/jacs.6b02155

[63] Van Der Heijden, A.E.D.M., & Bouma, R.H.B. (2004). Crystallization and characterization of RDX, HMX, and CL-20. *Cryst. Growth Des*., *4*, 999-1007. https://doi.org/10.1021/cg049965a

[64] Duan, B., Shu, Y., Liu, N., Wang, B., Lu, X., & Lu, Y. (2018). Direct insight into the formation driving force, sensitivity and detonation performance of the observed CL-20-based energetic cocrystals. *Cryst. Eng. Comm.*, *20*, 5790-5800. https://doi.org/10.1039/C8CE01132J

[65] Liu, Y., Li, S., Xu, J., Zhang, H., Guan, Y., Jiang, H., Huang, S., Huang, H., & Wang, Z. (2018). Three energetic 2, 2′, 4, 4′, 6, 6′-hexanitrostilbene cocrystals regularly constructed by H-bonding, π-stacking, and van der Waals interactions. *Cryst. Growth Des., 18*, 1940-1943.

[66] Zhang, C., Yang, Z., Zhou, X., Zhang, C., Ma, Y., Xu, J., Zhang, Q., Nie, F., & Li, H. (2014). Evident hydrogen bonded chains building CL-20-based cocrystals. *Cryst. Growth Des*., *14*, 3923-3928. https://doi.org/10.1021/cg500796r

[67] Thakuria, R., Nath, N.K., & Saha, B.K. (2019). The nature and applications of π-π interactions: A perspective. *Cryst. Growth Des*., *19*, 523-528. https://doi.org/10.1021/acs.cgd.8b01630

[68] Zhang, M., Tan, Y., Zhao, X., Zhang, J., Huang, S., Zhai, Z., Liu, Y., & Yang, Z. (2020). Seeking a novel energetic co-crystal strategy through the interfacial self-assembly of CL-20 and HMX nanocrystals. *Cryst. Eng. Comm*., *22*, 61-67. https://doi.org/10.1039/c9ce01447k

[69] An, C., Yu, B., Li, H., Guo, W., & Wang, J. (2015). Preparation and characterization of ultrafine ε-hexanitrohexaazaisowurtzitane particles. *nternational Journal of Energetic Materials and Chemical Propulsion*, *14*(4), 295-306. https://doi.org/10.1615/IntJEnergeticMaterialsChemProp.2015011266

[70] An, C., Li, H., Guo, W., Geng, X., & Wang, J. (2014). Nano cyclotetramethylene tetranitramine particles prepared by a green recrystallization process. *ropellants, Explosives, Pyrotechnics*, *39*(5), 701-706. https://doi.org/10.1002/prep.201300199

[71] Shi, X., Wang, J., Li, X., & An, C. (2015). Preparation and properties of HMX/Nitrocellulose nanocomposites. *Journal of Propulsion and Power*, *31* (2), 757-760. https://doi.org/10.2514/1.B35491

[72] Naya, T., & Kohga, M. (2013). Influences of particle size and content of HMX on burning characteristics of HMX-based propellant. *Aerospace Science and Technology*, *27*(1), 209-215. https://doi.org/10.1016/j.ast.2012.08.012

[73] Naya, T., & Kohga, M. (2014). Influences of particle size and content of RDX on burning characteristics of RDX-based propellant. *Aerospace Science and Technology*, *32*(1), 26-34. https://doi.org/10.1016/j.ast.2013.12.004

[74] Cai, H., Tian, L., Huang, B., Yang, G., Guan, D., & Huang, H. (2013). **1,1-**Diamino-2,2-dintroethene (FOX-7) nanocrystals embedded in mesoporous carbon FDU-15. Mesopor. Mat., 170, 20-25. https://doi.org/10.1016/j.micromeso.2012.11.034

[75] Majano, G., Mintova, S., Bein, T., & Klapotke, T.M. (2006). Confined detection of high-energy-density materials. *Adv. Mater.*, *18*, 2440-2443. https://doi.org/10.1021/jp068863n

[76] Yang, G., Nie, F., Huang, H., Zhao, L., & Pang, W. (2006). Preparation and characterization of nano-TATB explosive. *Propellants, Explos., Pyrotech., 31*, 390-394. https://doi.org/10.1002/prep.200600053

[77] Yang, G., Nie, F., Li, J., Guo, Q., & Qiao, Z. (2007). Preparation and characterization of nano-NTO explosive. *J. Energ. Mater.,* 25, 35-47. https://doi.org/10.1080/07370650601107104

[78] Bolton, O., & Matzger, A.J. (2011). Improved stability and smart-material functionality realized in an energetic cocrystal. *Angew. Chem. Int. Ed., 50*, 8960-8963. https://doi.org/10.1002/ange.201104164

[79] Sander, J.R., Bucar, D.K., Henry, R.F., Zhang, G.G., & MacGillivray, L.R. (2010). Pharmaceutical nano-cocrystals: Sonochemical synthesis by solvent selection and use of a surfactant. *Angew. Chem. Int. Ed., 49*, 7284-7288. https://doi.org/10.1002/ange.201002588

[80] Almarsson, O., & Zaworotko, M.J. (2004). Crystal engineering of the composition of pharmaceutical phases. Do pharmaceutical co-crystals represent a new path to improved medicines? *Chem. Commun.*, 1889-1896. https://doi.org/10.1039/B402150A

[81] Berry, D.J., Seaton, C.C., Clegg, W., Harrington, R.W., Coles, S.J., Horton, P.N., Hursthouse, M.B., Storey, R., Jones, W., Friscic, T., & Blagden, N. (2008). Applying

hot-stage microscopy to co-crystal screening: A study of nicotinamide with seven active pharmaceutical ingredients. *Cryst.Growth Des., 8*, 1697-1712. https://doi.org/10.1021/cg800035w

[82] Khan, M., Enkelmann, V., & Brunklaus, G., (2010). Crystal engineering of pharmaceutical co-crystals: application of methyl paraben as molecular hook. *J. Am. Chem. Soc.*, *132*, 5254-5263. https://doi.org/10.1021/ja100146f

[83] Brader, M.L., Sukumar, M., Pekar, A.H., McClellan, D.S., Chance, R.E., Flora, D.B., Cox, A.L., Irwin, L., & Myers, S.R. (2002). Hybrid insulin cocrystals for controlled release delivery. *Nat. Biotechnol.*, *20*, 800-804. https://doi.org/10.1038/nbt722

[84] Gao, B., Wang, D., Zhang, J., Hu, Y., Shen, J., Wang, J., Huang, Z., Qiao, B., Huang, H., Nie, F., & Yang, G. (2014). Facile, continuous and large-scale synthesis of CL-20/HMX nano co-crystals with high-performance by ultrasonic spray-assisted electrostatic adsorption method. *J. Mater. Chem. A*, *47*, 1-7. https://doi.org/10.1039/C4TA04979A

[85] Stepanov, V., Anglade, V., Balas Hummers, W.A., Bezmelnitsyn, A.V., & Krasnoperov, L.N. (2011). Production and sensitivity evaluation of nanocrystalline RDX-based explosive compositions. *Propellants, Explos., Pyrotech.*, *36*, 240-246. https://doi.org/10.1002/prep.201000114

[86] Doherty, R.M., & Watt, D.S. (2008). Relationship between RDX properties and sensitivity. *Propellants*, *Explos., Pyrotech., 33*(1), 13. https://doi.org/10.1002/prep.200800201

[87] Czerski, H., Greenaway, M.W., Proud, W.G., & Field, J.E. (2006). Links between the morphology of RDX crystals and their shock sensitivity. *AIP Conf. Proc.*, *845*, 1053-1056. https://doi.org/10.1063/1.2263503

[88] van der Heijden, A.E.D.M., Bouma, R.H.B., & van der Steen, A.C. (2004). Physicochemical parameters of nitramines influencing shock sensitivity. *Propellants, Explos., Pyrotech.*, *29*, 304-313. https://doi.org/10.1002/prep.200400058

[89] Spyckerelle, C., Eck, G., Sjoberg, P., & Amneus, A.M. (2008). Reduced sensitivity RDX obtained from Bachmann RDX. *Propellants, Explos., Pyrotech., 33*, 14-19. https://doi.org/10.1002/prep.200800202

[90] Millar, D.I.A., Maynard-Casely, H.E., Allan, D.R., Cumming, A.S., Lennie, A.R., Mackay, A.J., Oswald, I.D.H., Tang, C.C., & Pulham, C.R. (2012). Crystal engineering of energetic materials: Co-crystals of CL-20. *Cryst. Eng. Comm.*, *14*, 3742-3749. https://doi.org/10.1039/C2CE05796D

[91] Wang, Y., Yang, Z., Li, H., Zhou, X., Zhang, Q., Wang, J., & Liu, Y. (2014). A novel cocrystal explosive of HNIW with good comprehensive properties. *Propellants, Explos., Pyrotech.*, *39*(49), 590-596. https://doi.org/10.1002/prep.201300146

[92] Anderson, S.R., am Ende, D.J., Salan, J.S., & Samuels, P. (2014). Preparation of an energetic-energetic cocrystal using resonant acoustic mixing. *Propellants, Explos., Pyrotech.*, *39*(5), 637-640. https://doi.org/10.1002/prep.201400092

[93] Trask, A.V. (2005). Crystal engineering of organic cocrystals by the solid- state grinding approach. *Top. Curr. Chem.*, *254*, 41 -70. https://doi.org/10.1007/b100995

[94] Qiao, N., Li, M., Schlindwein, W., Malek, N., Davies, A., & Trappitt, G. (2011). Pharmaceutical cocrystals: An overview. *Int. J. Pharm., 419*(1-2), 1-11. https://doi.org/10.1016/j.ijpharm.2011.07.037

[95] Han, G., Li, Q-F., Gou, R-J., Zhang, S-H., Ren, F-D., Wang, L., & Guan, R. (2017). Growth morphology of CL-20/HMX cocrystal explosive: insights from solvent behavior under different temperatures. *Journal of Molecular Modeling 23*, 360. https://doi.org/10.1007/s00894-017-3525-3

[96] Jia, Q., Wang, J., Zhang, S., Zhang, J., Liu, N., & Kou, K. (2021). Investigation of the solid-liquid ternary phase diagrams of 2HNIW.HMX cocrystal. *RSC Adv*., *11*(16), 9542-9549. https://doi.org/10.1039/d1ra00057h

[97] Zhang, S., Zhang, J., Kou, K., Jia, Q., Xu, Y., Liu, N., & Hu, R. (2019). Standard enthalpy of formation, thermal behavior, and specific heat capacity of 2HNIW·HMX co-crystals. *J. Chem. Eng. Data*, *64*, 42-50. https://doi.org/10.1021/acs.jced.8b00454

[98] Zhang, S., Zhang, J., Kou, K., Jia, Q., Xu, Y., Zerraza, S., Liu, N., & Hu, R. (2019). Investigation on the dissolution behavior of 2HNIW.HMX co-crystal prepared by a solvent/non-solvent method in N,N-dimethylformamide at T = (298.15-318.15) K. *Journal of Thermal Analysis and Calorimetry, 135*, 3363-3373**.** https://doi.org/10.1007/s10973-018-7502-6

[99] Wang, K., & Zhu, W.H. (2020). Theoretical studies on the surface property, thermal behaviors, stability, and disassembly process of HMX/DMF cocrystal. *Comput. Mater. Sci., 178*, 109643. https://doi.org/10.1016/j.commatsci.2020.109643

[100] Jia, Q., Zhang, J., Zhang, S., Lei, D., Xu, Y., & Kou, K. (2019). Investigation of the phase behavior of a HNIW·TNT cocrystal system and construction of ternary phase diagrams. *Cryst. Growth Des.*, *19*, 6370-6376. https://doi.org/10.1021/acs.cgd.9b00845

[101] Alhalaweh, A., & Velaga, S.P. (2010). Formation of cocrystals from stoichiometric solutions of incongruently saturating systems by spray drying. *Cryst. Growth Des.*, *10*, 3302-3305. https://doi.org/10.1021/cg100451q

[102] Childs, S.L., Rodríguez-Hornedo, N., Reddy, L.S., Jayasankar, A., Maheshwari, C., McCausland, L., Shipplett, R., & Stahly, B.C. (2008). Screening strategies based on solubility and solution composition generate pharmaceutically acceptable cocrystals of carbamazepine. *Cryst. Eng. Comm., 10*, 856-864. https://doi.org/10.1039/b715396a

[103] Hong, C., Xie, Y., Yao, Y., Li, G., Yuan, X., & Shen, H. (2015). A novel strategy for pharmaceutical cocrystal generation without knowledge of stoichiometric ratio: Myricetin cocrystals and a ternary phase diagram. *Pharm. Res.*, *32*, 47-60. https://doi.org/10.1007/s11095-014-1443-y

[104] Veith, H., Schleinitz, M., Schauerte, C., & Sadowski, G. (2019). Thermodynamic approach for co-crystal screening. *Cryst. Growth Des.*, *19*, 3253. https://doi.org/10.1021/acs.cgd.9b00103

[105] Loschen, C., & Klamt, A. (2018). Cocrystal ternary phase diagrams from density functional theory and solvation thermodynamics. *Cryst. Growth Des.*, *18*, 5600-5608. https://doi.org/10.1021/acs.cgd.8b00923

[106] Jia, X., & Wang, J., (2019). Preparation and characterization of spherical submicron ε-CL-20 via green mechanical demulsification. *J. Energ. Mater.*, *37*, 475-483. https://doi.org/10.1080/07370652.2019.1651421

[107] Xu, X-J., Zhu, W-H., & Xiao, H-M. (2007). DFT Studies on the four polymorphs of crystalline CL-20 and the influences of hydrostatic pressure on ε-CL-20 crystal. *J. Phys. Chem. B*, *111*, 2090- 2097, https://doi.org/10.1021/jp066833e

[108] Bayat, Y., Zarandi, M., Zarei, M.A., Soleyman, R., & Zeynali, V. (2014). A novel approach for preparation of CL-20 nanoparticles by microemulsion method. *J. Mol. Liq.*, *193*, 83-86. https://doi.org/10.1016/j.molliq.2013.12.028

[109] Hudson, R.J., Moniruzzaman, M., & Gill, P.P. (2015). Investigation of crystal morphology and shock sensitivity of cyclotrimethylenetrinitramine suspension by rheology. *Propellants, Explos., Pyrotech.*, *40*, 233- 237. https://doi.org/10.1002/prep.201400129

[110] Guo, D., An, Q., Zybin, S.V., Goddard, W.A., Huang, F., & Tang, B. (2015). The co-crystal of TNT/CL-20 leads to decreased sensitivity toward thermal decomposition from first principles based reactive molecular dynamics. *J. Mater. Chem. A*, *3*,5409-5419. https://doi.org/10.1039/C4TA06858K

[111] Yang, Z-W., Zhang, Y-L., Li, H-Z., Zhou, X-Q., Nie, F-D., Li, J-S., & Huang, H.H. (2012). Preparation, structure and properties of CL-20/TNT cocrystal. *Hanneng Cailiao/Chinese Journal of Energetic Materials*. *20*. 674-679. https://doi.org/10.3969/j.issn.1006-9941.2012.06.003

[112] Cao, Q., Xiao, J.J., Gao, P., Li, S.S., Zhao, F., Wang, Y.A., & Xiao, H.M. (2017). Molecular dynamics simulations for CL-20/TNT co-crystal based polymer- bonded explosives. *Journal of Theoretical and Computational Chemistry*, *16*(8), 1750072. https://doi.org/10.1142/s0219633617500729

[113] Li, Y., Yu, W-Li, & Huang, H. (2022). CL-20/TNT decomposition under shock: cocrystalline versus amorphous. *RSC Adv*., *12*, 6938-6946. https://doi.org/10.1039/D1RA09120D

[114] Wang, J-Y., Li, H-Q., An, C-W., & Guo, W-J. (2015). Preparation and characterization of ultrafine CL-20/TNT cocrystal explosive by spray drying method. *Chinese Journal of Energetic Materials, 23*(11), 1103-1106. https://doi.org/10.16251/j.cnki.1009-2307.2015.11.013

[115] Hang, G.Y., Yu, W.L., Wang, T., & Wang J-T. (2019). Theoretical investigations on structures, stability, energetic performance, sensitivity, and mechanical properties of CL-20/TNT/HMX cocrystal explosives by molecular dynamics simulation. *J. Mol Model, 25*, 10 (2-15) . https://doi.org/10.1007/s00894-018-3887-1

[116] Chen, P.Y., Zhang, L., Zhu, S.G., & Cheng, G.B. (2015). Difference of mixing and cocrystallization of TNT and CL-20 studied by molecular dynamics simulation. *Applied Mechanics and Materials* (AMM), *703,* 215-219. https://doi.org/10.4028/www.scientific.net/amm.703.215

[117] Wang, F., Du, G., Zhang, C., & Wang, Q-Y. (2023). Mechanism of the impact-sensitivity reduction of energetic CL-20/TNT cocrystals: A nonequilibrium molecular dynamics study. *Polymers*, *15*(6), 1576. https://doi.org/10.3390/polym15061576

[118] Tan, Y., Yang, Z., Wang, H., Li, H., Nie, F., Liu, Y., & Yu, Y. (2019). High energy explosive with low sensitivity: A new energetic cocrystal based on Cl-20 and 1,4-DNI. *Cryst. Growth Des.*, *19*, 8, 4476-4482. https://doi.org/10.1021/acs.cgd.9b00250

[119] Hu, R.Z., Yao, E.G., Ma, H.X., Zhang, H., Gao, H.X., Han, L., Zhao, F.Q., Luo, Y., & Zhao, H.A. (2015). The empirical nitrogen equivalent equations for predicting the detonation velocity and detonation pressure of CHNO explosive with approaching the results of Kamlet-Jacobs equations. *Chin. J. Energy. Mater.*, 23,1243-1244. https://doi.org/10.11943/j.issn.1006-9941.2015.12.019

[120] Li, X., Song, L., Zhao, Y., & Ju, X-H. (2023). Crystal morphology prediction of CL-20 and 1,4-DNI co-crystal at different temperatures. *J. Mol. Model.*, *29*, 135. https://doi.org/10.1007/s00894-023-05528-1

[121] Dong, H-Y., Long, Yi-Q., Zhou, T-T., Wu, B., & Duan, X-H. (2020). Thermodynamic on

the formation of CL-20/1,4-DNI cocrystal. *Chinese Journal of Energetic Materials*, *28*(9), 819-825. https://doi.org/10.11943/CJEM2020057

[122] Xu, X., Zhang, R., Xia, W., Ma, P., Ma, C., Pan, Y., & Jiang, J. (2022). Density functional theory study of CL-20/Nitroimidazoles energetic cocrystals in an external electric field. *Computational and Theoretical Chemistry, 1209*, 113607. https://doi.org/10.1016/j.comptc.2022.113607

[123] Song, X., Wang, Y., An, C., Guo, X., & Li, F. (2008). Dependence of particle morphology and size on the mechanical sensitivity and thermal stability of octahydro-1,3,5,7-tetranitro-1,3,5,7-tetrazocine. *J. Hazard. Mater., 159*, 222-229. https://doi.org/10.1016/j.jhazmat.2008.02.009

[124] Song, X.L., & Li, F.S. (2009). Dependence of particle size and size distribution on mechanical sensitivity and thermal stability of hexahydro-1,3,5-trinitro-1,3,5-triazine. *Defence Science Journal*, *59*, 37-42. https://doi.org/10.14429/dsj.59.1482

[125] Radacsi, N., Bouma, R.H.B., Haye, E.L.M.K., ter Horst, J.H., Stankiewicz, A.I., & van der Heijden, A.E.D.M. (2013). On the reliability of sensitivity test methods for submicrometer-sized RDX and HMX particles. *Propellants, Explos., Pyrotech.*, *38*(6), 761-769. https://doi.org/10.1002/prep.201200189

[126] Bayat, Y., & Zeynali, V. (2011). Preparation and characterization of nanosized-CL-20 explosive. *J. Energetic Mater.*, *29*, 281-291. https://doi.org/10.1080/07370652.2010.527897

[127] Siviour, C.R., Gifford, M.J., Walley, S.M., Proud, W.G., & Field, J.E. (2004). Particle size effects on the mechanical properties of a polymer bonded explosive. *Journal of Materials Science*, *39*, 1255-1258. https://doi.org/10.1023/B:JMSC.0000013883.45092.45

[128] Luman, J.R., Wehrman, B., Kuo, K.K., Yetter, R.A., Masoud, N.M., Manning, T.G., Harris, L.E., & Bruck, H.A. (2007). Development and characterization of high performance solid propellants containing nano-sized energetic ingredients. *Prog. Combust. Inst.*, *31*(2), 2089 -2096. https://doi.org/10.1016/j.proci.2006.07.024

[129] Chavez, D.E., Tappan, B.C., Hiskey, M.A., Son, S.F., Harry, H., Montoya, D., & Hagelberg, S. (2005). New high-nitrogen materials based on nitroguanyl-tetrazines: explosive properties, thermal decomposition and combustion studies. *Propellants, Explos., Pyrotech.*, *30*(6) , 412 - 417. https://doi.org/10.1002/prep.200500033

[130] Sanghavi, R.R., Pillai, A.G.S., Velapure, S.P., & Singh, A. (2003). Studies on different types of nitrocellulose in triple base gun propellant formulations. *J. Energetic Mater.*, *21*(2), 87-95. https://doi.org/10.1080/713845496

[131] Damse, R.S., & Sikder, A.K. (2007). Role of inorganic additives on the ballistic performance of gun propellant formulations. *J. Hazard. Mater.*, *154*(1-3), 888-892. https://doi.org/10.1016/j.jhazmat.2007.10.103

[132] Lv, Q., & Feng, Q.L. (2006). Preparation of 3-D regenerated fibroin scaffolds with freeze drying method and freeze drying/foaming technique. *J. Mater. Sci: Mater. Med.*, *17*(12), 1349-1356. https://doi.org/10.1007/s10856-006-0610-z

[133] Wu, X., Liu, Y., Li, X., Wen, P., Zhang, Y., Long, Y., Wang, X., Guo, Y., Xing, F., & Gao, J. (2010). Preparation of aligned porous gelatin scaffolds by unidirectional freeze-drying method. *Acta Biomaterialia*, *6*(3), 1167-1177. https://doi.org/10.1016/j.actbio.2009.08.041

[134] Yin, Y., Wang, J., Chen, J., Sun J., & H Sui. (2022,). Thermal kinetics of energetic CL-20/BTF cocrystal ınduced by strong ıntermolecular coupling. *J. Phys. Chem. C*, *126*(19), 8199-8207. https://doi.org/10.1021/acs.jpcc.1c05812

[135] Hao, L., Wang J., Zhai, D., Ma, P., Ma, C., Pan, Y., & Jiang, J. (2020). Theoretical study on CL-20-based cocrystal energetic compounds in an external electric field. *ACS Omega*, *5*(24), 14767-14775. https://doi.org/10.1021/acsomega.0c01643

[136] Li, S.S., Li, Q.L., & Xiao, J.J. (2023). DFT study for effects of hydrostatic pressure on structure, interaction and mechanical properties of CL-20/BTF cocrystal. *Cryst. Eng. Comm.*, *25*, 5966-5974. https://doi.org/10.1039/D3CE00680H

[137] Hamilton, B.W., Steele, B.A., Sakano, M.N., Kroonblawd, M.P., Kuo, I.-F. W., & Strachan, A. (2021). Predicted reaction mechanisms, product speciation, kinetics, and detonation properties of the insensitive explosive 2,6-diamino-3,5-dinitropyrazine-1-oxide (LLM-105). *The Journal of Physical Chemistry A, 125*(8), 1766-1777. https://doi.org/10.1021/acs.jpca.0c10946

[138] Zhang, S.H., & Zhao, H.L. (2014). Preparation and characterization of LLM-105 cocrystal explosives. *Advanced Materials Research*, *900*, 251-255. https://doi.org/10.4028/www.scientific.net/amr.900.251

[139] Hang, Gy., Wang, Jt., Wang, T., Shen, H-M., & Yu, W-L. (2022). Theoretical investigations on a novel CL-20/LLM-105 cocrystal explosive by molecular dynamics method. *Theor. Chem. Acc., 141*(23), https://doi.org/10.1007/s00214-022-02886-6

Glossary

AIM : Atoms in molecules

ARC : Accelerating rate calorimeter

BDEs : Bond dissociation energies

BTF : Benzotrifuroxan

CED : Cohesive energy density

CL-20 : Hexanitrohexaazaisowurtzitane

CL-20 : 2,4,6,8,10,12-Hexanitro-2,4,6,8,10,12-hexaaza-tetracyclo-[5.5.0.05,9.03,11]-dodecane

DFT : Density functional theory

1,4-DNI : 1,4-Dinitroimidazole

DSC : Differential scanning calorimetry

EMs : Energetic materials

ECCs : Energetic cocrystals

ESPs : Electrostatic potentials

FMRs : Five member rings

HE : High explosive

HEDC : High energy density compound

HEMs : High energy materials

HMX : 1,3,5,7-Tetranitro-1,3,5,7-tetrazacyclooctane (HMX)

HINIW : 2,4,6,8,10,12-Hexanitro-2,4,6,8,10,12-hexaaza-tetracyclo-[5.5.0.05,9.03,11]-dodecane

IPA : Isopropanol

LEMs : Low energy materials

MD : Molecular dynamics

4,5-MDNI : 1-Methyl-4,5-dinitro-1H-imidazole

MSD : Mean square displacement (MSD)

NQ : Nitroguanidine

NPT : Constant pressure and temperature

NVT-MD : Constant volume and temperature molecular dynamics

OB : Oxygen balance

PBXs : Polymer-bonded explosives

RMD : Reactive molecular dynamics

PCFs : Pair correlation functions

PS : Polystyrene

PVAc : Polyvinyl acetate

PXRD : Powder X-ray diffraction

RDF : Radial distribution function

RDX : Hexahydro-1,3,5-trinitro-1,3,5-triazine

SCXRD : Single-crystal X-ray diffraction

SEM : Scanning electron microscopy

USEA : Ultrasonic spray-assisted electrostatic adsorption